2003

Precipitate growth features in the duplex size Gamma Prime distribution in the superalloy IN738LC

Indranil Roy
Louisiana State University and Agricultural and Mechanical College, iroy1@lsu.edu

PRECIPITATE GROWTH FEATURES IN THE DUPLEX SIZE GAMMA PRIME DISTRIBUTION IN THE SUPERALLOY IN738LC

A Thesis

Submitted to the Graduate Faculty of the
Louisiana State University and
Agricultural and Mechanical College
in partial fulfillment of the
requirement for the degree of
Master of Science in Mechanical Engineering

in

The Department of Mechanical Engineering

by
Indranil Roy
Bachelor of Engineering, Bengal Engineering College, India 1996
December 2003

Dedication

I give recognition and thanks to GOD for ordering my steps. This thesis is dedicated to the memory of my late father, Amitabha Roy (February 12, 1943 – January 30, 2000), my mother, Deepa Roy and my beloved wife Madhuchhanda Roy for her patience and loyal support.

Acknowledgements

I would like to express my sincere gratitude to my advisor, Dr. Aravamudhan Raman, for his continued advice, tenacious supervision and encouragement throughout the course of my research. I have learned much more than engineering of materials, heat treatment, and physical metallurgy from him. I appreciate his penetrating scientific approach that he conveyed to me and would like to acknowledge his scholastic expertise. I am indebted to him for his invaluable guidance and patient support.

This research would not have been complete without the help of Dr. Samuel Ibekwe, who contributed immensely, allowing me to use the very essential equipment available at Southern University. I am obliged to him for his valuable guidance. I am also grateful to Dr. Wen Jin Meng for teaching me Material Thermodynamics, indoctrinate the essentials of Material Characterization and TEM and also for allocating his time for priceless discussions. I thank Dr. Xiaogang Xie, High Magnification Imaging and Microanalysis Laboratory, Geology and Geophysics department, for training me to be proficient in image analysis using their SEM and allowing me to use their facilities for my research. Thanks are also gratefully extended to Dr. Tryfon T. Charalampopoulos for teaching me the fundamentals of LASER processing with material applications and for the thesis previewing. Special thanks are owed to Dr. M.M. Khonsari who gave me a great deal of insight into Thermal Engineering and Tribology.

Last, but not least, I would like to gratefully acknowledge partial project support from NASA through a DGAP grant No. NASA (2000-01)-DGAP-08, and a LaSpace grant No. NASA / LEQSF (2001-2005) - LASPACE, sponsored through the LA Board of Regents and LaSPACE consortium.

Table of Contents

List of Tables

List of Figures

List of Nomenclature

IN738LC	A cast Ni-base superalloy strengthened by γ' precipitates, containing low carbon; patented trademark of International Nickel Co., USA.
$L1_2$	FCC superlattice of the Cu_3Au type
$\Gamma_{\gamma\gamma'}$	γ - γ' interface energy
ε	Constrained lattice misfit
δ	Unconstrained lattice misfit parameter
K_p	Bulk modulus of the precipitate
G_m	Shear modulus of the matrix
γ'	$Ni_3Al(Ti, Nb)$ precipitate phase in a Ni-base superalloy with $L1_2$ structure
LSW	Lifshitz – Slyozov and Wagner theory
APB	Anti Phase Boundary
FC	Furnace-cooled
AC	Air-cooled
AAC	Accelerated air-cooled
WQ	Water quenched
HIP ing	Hot isostatic pressing
SEM	Scanning electron microscope
Q	Activation energy
PAM	Particle agglomeration mechanism
PBM	Particle break-up mechanism

Abstract

IN738LC is a modern, nickel base superalloy utilized at high temperatures in aggressive environments. Durability of this superalloy is dependent on the retention of strengthening by γ′ precipitates.

The precipitate growth features in the duplex size (fine and coarse) precipitate distribution was studied by heating the alloy for various times in vacuum at selected temperatures in the range 800 °C to 1100 °C. Increasing the holding times from 1 hour to 100 hours shows joining of the fine particles to form bigger particles, leading to distinct raft patterns. Two different γ′ precipitate growth processes had been observed: merging of smaller precipitates to produce larger ones (in duplex precipitate-size microstructures) that is, both the fine and the coarse precipitate particles grow with time, apparently by the particle movement in the matrix and coalescence – by the particle agglomeration mechanism (PAM), and growth through solute absorption from the matrix (Ostwald Ripening).

At 1100 °C the fine particles grew to the size of the coarse particles in about 100 hours and a single coarse size of about 840 nm was obtained. The activation energies for the growth of both the fine and coarse particles decrease with increase in temperature and size of the particles indicating that the coarser particles require less activation energy for the growth than the finer particles. This is attributed to the greater attractive force with which the coarser particles would attract the finer particles, in the overlapping diffusion zone thus requiring less activation energy for the growth. The activation energy for the precipitate growth in the duplex size range also was found to decrease progressively with increasing particle size at a given high temperature.

Chapter 1. Introduction

1.1 General

Superalloys belong to an important class of complex materials that exhibit high strength and oxidation resistance at elevated temperatures from 650 ^{o}C to 1100 ^{o}C in aggressive atmospheres as found in high temperature catalytic reactors, gas turbines, etc., and have made much of prevalent high temperature engineering possible **[1]**. They can be divided into three broad classes: Ni-base superalloys, Co-base superalloys and Fe-base superalloys. Ni-base superalloys have found widespread applications because of their excellent corrosion resistance, high strength coupled with ductility, creep and fatigue resistance, optimal impact and wear resistance and capability of offering excellent physical and mechanical properties at high temperatures. The γ' phase is the key factor responsible for the extraordinary, useful high temperature properties. This phase that has an ordered superlattice structure precipitates out of the matrix coherently and provides precipitate hardening.

IN738LC is an investment casting superalloy, which is frequently used for high temperature applications, especially for buckets and blades in stationary gas turbines **[2]**. Mechanical properties of this alloy are well known at high temperatures. Solid solution strengthening of the FCC γ Ni-base matrix and dispersion of the γ' Ni_3Al (Ti, Nb) intermetallic precipitate phase having the ordered FCC $L1_2$ structure (ordered structure of the Cu_3Au-type, wherein Ni atoms occupy the centers of the cube faces and the (Al, Ti) atoms the corners of the cube) with suitable shape, size and volume fraction in it results in the useful properties of IN738LC. The γ' phase in general has a coherency relationship

with the matrix **[3]**. Good thermal stability of the desired microstructure is achieved by minimizing the g/g' misfit (and hence the interfacial misfit energy). The chemical composition of many wrought nickel base superalloys are controlled to provide very high volume fractions of γ′ precipitates (up to 0.75), and the formation of γ′ during commercial heat treatments generally involves very high nucleation densities. The precipitate morphology achieved, therefore, is frequently related to the coarsening behavior of the γ′ phase, since the full volume fraction is attained very early in the thermal history of the material **[3]**.

Thus the successful utilization of the superalloy IN738LC is dependent on its microstructural stability; hence, microstructure control and stabilization is very necessary when the alloy is used at high temperatures. Properties of this superalloy with the microstructure having developed a duplex size distribution of the γ′ precipitates are governed by the variations in the microstructure. It has been observed that increasing the holding times from 1 hour to 100 hours shows agglomeration of the fine particles to form bigger particles, as well as joining of fine particles with the nearby coarser particles, eventually leading to rafting. (Rafting refers to alignment of adjacent particles along low energy, <100> directions and later their joining with each other forming linear chains).

1.2 The g and g ¢ Phases

Both the γ and γ′ phases have the FCC crystal structure. The γ′ phase is long range ordered and coherent with the matrix γ phase. Two distinct atomic positions involved are:

1. Face centers of the FCC elemental cells.
2. Corner positions of the FCC elemental cells.

γ' has the crystal structure of the ordered Cu_3Au phase and this ordered superlattice is designated $L1_2$. In the binary ordered Ni_3Al - γ' phase, Ni occupies the face centers, while Al occupies the corner positions. In multiple component γ' phases, the face centers and the corner atoms have to be characterized experimentally. Karg, *et. al.* **[4]** delved into this for various commercial and experimental alloys. The authors stated that heat treatments below 1363 ^oK do not significantly affect the distribution of the elements in their respective sites. Since the γ and γ' interface is coherent, the interface energy $\Gamma_{\gamma\gamma'}$ (per unit area) is small, which ensures homogeneous nucleation of the γ' phase.

It is to be noted that the fine coherent γ' precipitates embedded in the γ matrix are normally constrained. They are forced to adjust their lattice constants somewhat to that of the matrix. The relative difference in the lattice constant of such constrained particles is called the constrained lattice misfit ε. If a_γ and $a_{\gamma'}$ are the unconstrained lattice constants of the respective phases, the unconstrained lattice misfit parameter δ is defined as:

$$\delta = (a_\gamma - a_{\gamma'}) / a_\gamma \quad \text{……………………………………(1)}$$

Mott and Nabarro **[5]** related ε to δ, the bulk modulus K_p of the precipitate and the shear modulus G_m of the matrix **[6]**.

$$\varepsilon = \delta / \{1+ 4G_m/3K_p\} \quad \text{……………………………(2)}$$

1.3 The Role of Alloying Elements in the Design of the Superalloy

A few of the vast number of reviews have been published on the defect structure and precipitate defect interactions **[7]**, microstructural characteristics **[8]**, and structure property relations **[9]** in nickel base superalloys. Since the publication of these reviews there has been considerable progress in the understanding of the role of the various

constituents of Ni-base superalloys. The constituents of Ni-base superalloys have been classified into solid solution formers, precipitate formers, carbide formers and surface stabilizers. The role of each constituent element has been critically assessed. The precipitate formers have been analyzed and the occurrence of Ni_3X type compounds, their structure, crystallography of their precipitation, role of alloying additions on the coherency of these precipitates, etc., have been considered **[10]**.

1.4 Hardening of Ni-base Superalloys

The strength of a Ni-base superalloy, hardened through precipitation, is related to volume fraction and distribution of the γ' intermetallic precipitate phase and the γ' particle size **[11].** These parameters are the result of high temperature services or various heat treatment processes. The knowledge of the influence of time and temperature on the γ' precipitate phase is of prime importance due to the technological application of the superalloys at high temperatures. Precipitation or dissolution mechanisms are such that the volume fraction balance of the γ' precipitate phase is quickly established at an ageing temperature, successive changes being only to particle growth. These parameters can be controlled by varying the heat treatment parameters **[12]**. The theory of controlled growth of particles through diffusion has been formulated by Lifshitz and Slyozov **[13]** and by Wagner **[14]**, known as the combined LSW theory (the volume fraction of γ' varying between 9 to 75 %). In this case the driving force of the precipitate growth is the decrease of the precipitate overall superficial energy **[15].** The LSW theory predicts that the average radius, r, of an equimaxed particle would increase in time, t, according to the equation:

$$(r^3 - r_0^3)^{\frac{1}{3}} = K t^{\frac{1}{3}} \quad \text{……..……..(3)}$$

where "r_o" is the particle size before growth starts. The rate constant, K, is given by:

$$K = \frac{2\gamma D C_e V_m^2}{\rho_c^2 RT} \quad \text{……..…….(4)}$$

where γ is the interfacial energy between the precipitate and the matrix, D is the solute diffusion coefficient in the matrix and is given by:

$$D = D_0 \exp\left(-\frac{Q}{RT}\right), \text{ where Q is the diffusion activation energy……..…(5)}$$

C_e is the concentration of the solute balanced with a precipitate of radius ∞, V_m is the molar volume of the precipitate, ρ_c is a numerical constant related to the precipitate distribution size, R is the universal gas constant and T is the absolute temperature. The first growth theories were developed by Greenwood **[16]** for small volume fractions of the γ' precipitate phase. The LSW theory is also applicable when the γ' volume fraction is small. It is to be noted that when the volume fraction of γ' is large the diffusion distance becomes shorter. The effect of volume fraction on the precipitate growth was treated theoretically by Ardell **[17]**. It has been observed that the larger the volume fraction of the precipitate, the bigger is the particle. Ardell **[18]** has demonstrated that coarsening of the γ' in the Ni-Al and Ni-Cr-Al systems follows a diffusion-controlled model in which LSW theory is obeyed. However the coarsening rate has been shown **[19]** to be independent of the γ' volume fraction.

1.4.1 Induction Ageing of IN738LC

Influence of induction heating on IN738LC was investigated **[20]** and it was observed that desirable characteristics of the γ' precipitates was achieved in induction ageing at lower time and temperature in comparison with times and temperature of other types of ageing. Improvement of the microstructure obtained in induction ageing was related to the existence of an external electromagnetic force produced by induction current. This electromagnetic force raised the effective driving force necessary for the age hardening process and intensified the nucleation and growth of the γ' precipitates.

1.4.2 g ¢ Precipitate Particle Coarsening

The review paper by Jayanath and Nash **[21]** deals with the factors affecting particle-coarsening kinetics and size distribution and delves into the theories governing these phenomena. The LSW theory **[13, 14]** was developed to model kinetics of precipitate growth from supersaturated solid solutions. The theory corresponds to a zero volume fraction approximation, but has been modified for finite volume fractions in order to correspond to real situations. The LSW theory predicts the average particle volume to increase linearly with time and also predicts an asymptotic particle size distribution resulting from coarsening. In the LSW theory, Zener's approximation was adopted for the diffusion geometry, i.e., the growth rate is given by:

$$\frac{dr}{dt} = \frac{D(C - C_r)}{r} \qquad \text{.....(6)}$$

Here C is the concentration of the solute in the matrix in equilibrium with a particle of infinite radius. The above approximation becomes poor as the inter-particle distance decreases, corresponding to an increasing volume fraction, because the diffusion

field begins to overlap. In many commercial alloys second phase volume fractions of approximately 60 % are encountered. Thus the volume fraction effect is of considerable importance. Ardell **[17]** proposed a modification of the LSW theory by modifying the diffusion equation to take into account the volume fraction, using more realistic diffusion geometry. Many other theories **[22-26]** approached the problem of multi particle diffusion and accounted for the volume fraction of second phase particles with a basic approach. However, none of these theories takes into account particle coalescence. Coalescence is a volume fraction effect in addition to the overlap of diffusion fields. The effect of coalescence between particles has been investigated by David, et al. **[27, 28]** based on the theoretical treatment outlined by Lifshitz and Slyozov **[13]** and this modification is termed Lifshitz – Slyozov Encounter Modified theory (LSEM). It is assumed that coalescence occurs instantaneously when two particles encounter, i.e., two particles are removed from the smaller size range in the distribution and one is added to the larger size range. Coalescence is important in liquid-matrix systems, but is reduced in solid-state systems because of matrix strains around precipitates. In solid state systems with particles having ordered structures, coalescence might lead to the formation of APBs (Anti Phase Boundaries), which generally have much larger interfacial energies than particle / matrix interfaces.

1.4.3 g ¢ Precipitate Particle Coalescence

At high volume fractions the possibility of coalescence or encounters of two adjacent precipitate particles is very high. This phenomenon has been observed in both solid phase systems **[19, 27]** and liquid phase systems **[29, 30]**. There is some controversy over the physical mechanism of encounters. Davies, et al. **[27]** proposed that

if two precipitate particles are close enough to each other they coalesce forming one particle. Essentially it involves the overlapping of diffusion fields of the precipitate particles, but not necessarily physical contact in the initial stages. Once the particles have coalesced, the resulting particle shape is then considered to change rapidly to the equilibrium shape by particle/matrix surface diffusion. According to Doherty **[31]** coalescence occurs when the particles attract each other and move together. The driving force of this attraction is the removal of the elastically strained matrix between the two precipitates due to lattice parameters of the precipitate and matrix being different, i.e., the process depends on lattice mismatch. Doherty **[31]** substantiated his model of coalescence by referring to the results of Rastogi and Ardell **[32]** in which they found that as the lattice mismatch increased there was an increase in the maximum observed radius value and also the PSD (particle size distribution) broadening. It is to be noted that the LSEM theory models the coalescence events independent of the exact mechanism by which it occurs, because the interaction volume for coalescence is a variable which may simply be increased, if there is a longer range interaction as assumed by Lifshitz and Slyozov **[13]** and Davies, et al. **[27]**. A different mechanism of coalescence has also been proposed in liquid phase sintered systems. Kang and Yoon **[30]** proposed that when the grains touch each other, the coalescence of grains takes place by a migration of the grain boundary between them towards the smaller grain. This may be due to the rapid diffusion along the particle/matrix interface as soon as a neck is formed between the two grains. Kang and Yoon **[29]** observed that the activation energy for coarsening remained constant with change in volume fraction, indicating that the dominant mechanism for

coarsening of grains is still volume diffusion through the matrix even though the particles are touching each other.

1.4.4 Long Time Growth of g ¢ Precipitates in IN738LC

In IN738LC, after initial heat treatment resulting in the presence of two distinct γ′ precipitate populations **[33]**, the variation with cube root of exposure time of the γ′ precipitate size has been reported to be complex. On ageing, it has been observed that the mean size of the larger population of primary particles remained fairly constant at a value of about 0.35 μm, whilst that of the smaller size population of secondary particles increased. The rate of coarsening of the secondary particles making up the duplex γ′ precipitate morphology was seen to be dependent on the ageing temperature. Subsequent growth of the primary particles occurred only when the overall size distribution appeared to be unimodal and the growth obeyed the $t^{\frac{1}{3}}$ law. The maximum size attained by the secondary particles has been observed to be about 0.15 – 0.17 μm, and further ageing resulted in their rapid disappearance. The change in size of the primary particles has been considered to be closely related to a change in shape. The original heat treatments **[33]** resulted in cuboidal precipitates (0.35 μm in size) consequent to the high degree of mismatch between the matrix and the γ′ precipitate phase, but on initiation of the growth of the γ′ precipitates, they transformed to roughly spheroidal particles.

The driving force for the growth of the primary particles has been stated to be the reduction in the total mismatch strain and this process is said to be operative only when the secondary solute particles have attained a size and surface concentration comparable with those of the primary particles (0.15 – 0.17 μm in size). Subsequently the essentially

single size population experiences normal growth kinetics. As the growth proceeds, ageing changes the matrix composition and hence decreases the mismatch and promotes spheroidization, (**Figures 1 and 2**) **[33],** with which our experimental results, concur.

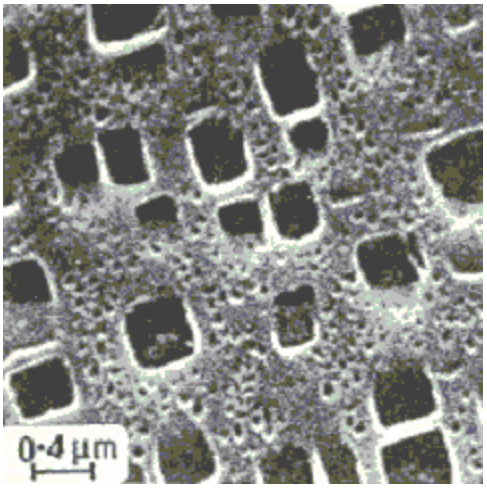

Figure 1: Microstructure of IN738LC after annealing for 360 hours at 750 °C.

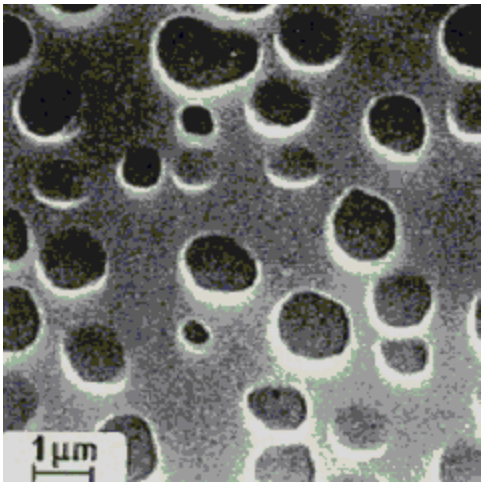

Figure 2: Microstructure of IN738LC after annealing for 15,000 hours at 750 °C.

1.4.5 Characteristics of the γ′ Precipitates and Influence of Various Heat Treatments in IN738LC

As in other Ni-base superalloys, γ′ precipitates in IN738LC contribute to strengthening of this alloy at high temperatures. In the study by Balikci and Raman **[34]**, the authors investigate the characteristics and mechanisms of the γ′ precipitate dissolution into the matrix solid solution. It has been observed that the γ′ precipitates grow in single size particles of cuboidal shape up to 1130 °C, above which precipitate dissolution leads to a duplex-size precipitate microstructure upon quenching from the temperature range 1140–1150 °C. The duplex-size precipitate microstructure is seen to consist of two very distinct sizes of precipitates (fine and medium coarse). It is observed that holding for longer times in the temperature range 1140–1150 °C does not coarsen the

fine precipitates of the duplex microstructure. Thus the source for the formation of the fine precipitates in the duplex microstructure is said to be the dissolution of the newly grown smaller-sized precipitates when the annealing starts from fine size precipitates and the "corner dissolution" of coarse precipitates when the starting microstructure consists of the maximum-sized cuboidal precipitates. At and above 1160 °C, the duplex as well as the coarse precipitate microstructures are seen to dissolve totally into the matrix to form a single-size fine precipitate microstructure of size 70 nm upon quenching from any temperature up to 1225 °C. A single-phase solid solution with no precipitates has been obtained only upon quenching from 1235 °C or above. The dissolution of coarse precipitates and formation of the fine ones are found to be very fast processes in the corresponding temperature ranges. The fine precipitates are postulated to form during quenching from the temperature range 1140–1225 °C and are considered to be of the "cooling" type.

The microstructure development of IN738LC has also been studied by Balikci and Raman **[35]**. As detailed in the literature, 1120 °C / 2h / AAC (accelerated air cooling) solution treatment produces a bimodal precipitate microstructure, which is not an adequate solutionizing procedure to yield a single-phase solid solution in the alloy. It has been detailed in **[35]** that 1235 °C / 4h / WQ (water quenched) solution treatment does produce a supersaturated single-phase condition. A microstructure with fine precipitates is observed to develop if solutionizing is carried out as 1200 °C / 4h / AAC. Ageing at lower temperatures after 1200 °C / 4h / AAC or WQ promotes precipitate growth in single size mode. Annealing below ~ 950 °C for 24 hours yields nearly spheroidal precipitates, while single ageing for 24 hours at 1050 °C or 1120 °C produces

single size cuboidal precipitates. Two different γ′ precipitate growth processes were observed: merging of smaller precipitates to produce larger ones in duplex precipitate size microstructure (particle agglomeration mechanism) and growth through solute absorption from the matrix (Ostwald Ripening). The average activation energies for the growth processes has been reported as 191 kJ/mole and 350 kJ/mole in the ranges of 850 °C to 1050 °C and 1050 °C to 1120 °C, respectively, for the latter process.

1.5 Microstructure Development

IN738LC is a Ni-base polycrystalline low carbon superalloy. Like other superalloys, IN738LC owes its exceptional properties to its FCC Ni-rich matrix strengthened by the γ′ Ni_3(Al, Ti) precipitate phase with the $L1_2$ superlattice structure. This alloy is investment cast and has about 40 - 43 % γ′ Ni_3Al(Ti, Nb) intermetallic precipitate phase in Ni-rich solid solution matrix **[36-42]**. This superalloy was patented in 1969 by C. G. Bieber and J.J. Galka **[43]**, assignors to the International Nickel Company, Inc., NY.

The microstructure of the IN738LC alloy with the matrix (FCC) phase and the duplex size γ′ precipitate phase particles are shown in **Figure 3**. The single phase γ′ Ni_3Al persists with the long-range order upto its melting point of 1380 °C, which is still above the liquidus range (1340 – 1375 °C) of IN738LC **[44]**. It has been observed from microstructural studies that negligible amounts of fine $M_{23}C_6$-type carbide at grain boundaries and large block MC-type carbides at the grain boundaries as well as in the matrix are present in the alloy.

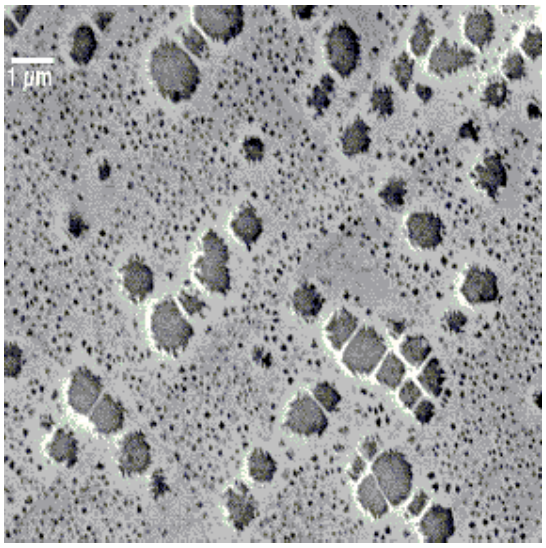

Figure 3: Microstructure of the g ¢ precipitated IN738LC alloy showing duplex precipitate size distribution. The fine particles are 'cooling precipitates'.

Carbide formation during different cooling rates from the melt was studied by Liu, et al. **[45, 46]**. It has been reported from their work that slow cooling rates produce more of large block MC carbides, and carbide refinement was observed with fast cooling rates and after cooling from temperatures close to 1595 °C, which is far above the melting range (1340 – 1375 °C) of carbides.

IN738LC is investment cast and often HIPed (Hot Isostatic Pressed) to remove microporosity. Due to HIPing, which is carried out at a temperature of about 1200 °C in a neutral atmosphere, the superalloy is likely to be solution treated. The standard commercial ageing treatment for IN738LC consists of two steps:

- Solutionizing
- Ageing

The solution treatment is carried out at 1200 °C for 2 hours and then cooling to room temperature usually by the process of accelerated air cooling (AAC) (blowing air) or by water quenching (WQ). Reheating the material to 850 °C and holding for 24 hours and furnace cooling (FC) thereafter to room temperature is the industry standard ageing treatment. This ageing process produces a bimodal γ' precipitate microstructure consisting of a cuboidal (approximately 450 nm) and spheroidal (approximately 80 nm) precipitate morphology **[47]**.

To suppress the formation of spheroidal precipitates and to obtain a unimodal-cuboidal precipitate microstructure, other heat treatment processes have been developed. The heat treatment sequence is a proper solution treatment followed by a combination of two-step ageing. As per industry standard, solution treatment is carried out at a temperature of 1120 – 1250 °C for 2 to 4 hours, followed by the first ageing being carried out at a temperature in the range 950-1100 °C. Subsequently the superalloy is cooled down to the second ageing temperature of about 650 – 950 °C for a time period and later cooled to room temperature. A variety of holding times of 12 to 200 hours have been reported in the literature for both the ageing treatments and also different cooling rates are detailed for either of the treatments.

It has been observed that with slow cooling rates subsequent to final ageing, spheroidal precipitates tend to become unimodal cuboidal with long periods of ageing times of about 100-200 hours at around 1000 °C **[42, 48]**. To understand the coarsening features of the second phase precipitate particles, a number of experimental and theoretical studies have been carried out **[27, 31, 48-68]**. The precipitate evolution process contributing to the minimization of the total free energy of the system, having

two contributing factors, the interfacial energy and the elastic strain energy, as well as the coarsening behavior of positively or negatively misfitting precipitates in the matrix, has been considered. It has been observed and postulated that the elastic strain energy due to the elastic self-energy and the configurational energy of the particles may be responsible for coarsening of the precipitates. In the early coarsening stage, the interfacial energy dominates the morphological evolution, and later, when the precipitates reach a critical size, the elastic strain energy takes over. Directional alignment of the coarsening precipitates along the elastically soft <100> direction in the Ni alloy system has been observed and ascribed to the tendency of the system to minimize its free energy.

It is necessary to note that only through thermo-mechanical treatments it is possible to obtain a refined grain distribution in a metallic material. Normal thermo-mechanical processes yield a recrystallized microstructure having reduced grain size through the interactions between grain boundaries and precipitates **[69]**. Any subsequent microstructure modification is mainly affected by the dissolution or reformation of the precipitates. Thermal Cycling is a recently developed method to obtain refined microstructure. The grain size reduction in this method is owed to the grain boundary and precipitate interactions **[70]**. A method of thermal cycling treatment was reported to have produced a microstructure whose grain size was half that of the original. It has been also reported that grain boundary liquidation can arrest the grain growth, evolving a reduced grain size **[71]**. Formation of fine subgrains (mosaic) during the annealing process is also well known **[72]**.

Second phase precipitate dissolution has been an issue for a long time. For the dissolution of precipitates into the matrix, different mechanisms have been proposed, as

for example, the interactions and concentration gradient in the precipitate – matrix interface to account for the dissolution of the precipitate phase **[73]**. A three-step model for second phase particle dissolution involving decomposition of the particles, crossing of the boundary and long distance diffusion has been proposed **[74]**. The importance of interface interactions as rate controlling processes for the dissolution of the single phase γ' Ni_3Al precipitates has been emphasized.

1.6 Research Motivations and Objective

Microstructure control and stabilization is very necessary for the effective utilization of the superalloy IN738LC at high temperatures. Developing suitable processes to reduce the grain size of the parent phase and to prevent the matrix grain and precipitate growths to improve the mechanical properties of the material are important in industrial applications. The current study focuses on the stability of the duplex size γ' precipitate microstructure in the alloy.

A standard heat treatment that is generally applied in the industry to IN738LC, is a solution treatment at 1120°C/2 h/WQ and a subsequent aging treatment at 850 °C/24 h/FC. This treatment gives the duplex size distribution for the γ' precipitates in the matrix. A microstructure with fine γ' precipitates develops if the treatment is carried out as 1200 °C/2 h/AAC. Annealing at lower temperatures after 1200 °C/4 h/AAC or WQ conditions leads to precipitate growth. Aging at 1120°C/24 h/WQ produces coarse size γ' precipitates. Further heating of the above specimens at 1140°C/6 h/WQ leads to partial dissolution of the coarse precipitates and produces a duplex microstructure by forming fine 'cooling precipitates' upon quenching **[75, 77]**.

Furnace cooling from 1200 °C showed joining of the fine particles to form bigger particles. Annealing of fine precipitate containing specimens at high temperatures led to their coarsening in single size mode and eventually to alignment of particles at some stage, causing the slow evolution of raft-like patterns. Two different γ′ precipitate growth processes were observed in general merging of smaller precipitates with adjacent smaller or larger precipitates by migration in the matrix (precipitate agglomeration, seen commonly in the duplex-size precipitate microstructure) **[35]** and growth through solute absorption from the matrix (Ostwald Ripening) **[35, 75, 76]**.

The growth characteristics of the γ′ precipitate in the duplex size (fine and medium) distribution have not been studied. The current research takes up this issue and analyzes the simultaneous growth features of both the fine and the medium size precipitate particles in the duplex size microstructure, when the alloy samples with the duplex size precipitates are heated for different lengths of time at temperatures in the range of 800 °C to 1100 °C.

The work presented in this thesis provides the basic data on the precipitate growth features in the duplex size γ′ distribution in the superalloy IN738LC, only.

Chapter 2. Experimental Background and Procedures

2.1 Materials

The material used in this study is the cast Ni-base polycrystalline, low carbon superalloy IN738LC. This material was provided by Howmet Corporation, Whitehall, MI in the form of rods with 15 mm diameter and 110 mm length. The investment cast rods were HIPed (Hot Isostatic Pressed) at 1185 °C for 2 hours to remove microporocity and then cooled to room temperature. The whole process was done in a neutral atmosphere. After the HIPing process the superalloy was solution treated at 1120°C for 2 hours, followed by an Argon backfill cooling to room temperature, with a cooling rate equivalent to air cooling. Annealing was carried out at 843°C for 24 hours, followed by an argon backfill cooling to room temperature. HIPing and ageing was carried out by the company that supplied the material. The chemical composition of the as-received material is given in **Table 1** and its precipitated microstructure is shown in **Figure 4**.

Table 1 Chemical Composition of As-Received IN738LC

Element	Ni	Cr	Co	Mo	W	Ta	Nb	Al	Ti	B	Zr	C
Wt %	Balance	15.7 to 16.3	8.0 to 9.0	1.5 to 2.0	2.4 to 2.8	1.5 to 2.0	0.6 to 1.1	3.2 to 3.7	3.2 to 3.7	0.007 to 0.012	0.03 to 0.08	0.09 to 0.13

2.2 Microstructure Development and Characterization

For the various heat treatments carried out during the course of this research, the above mentioned 15 mm diameter and 110 mm long rods of cast Ni-base polycrystalline, low carbon superalloy IN738LC was cut into thin slices.

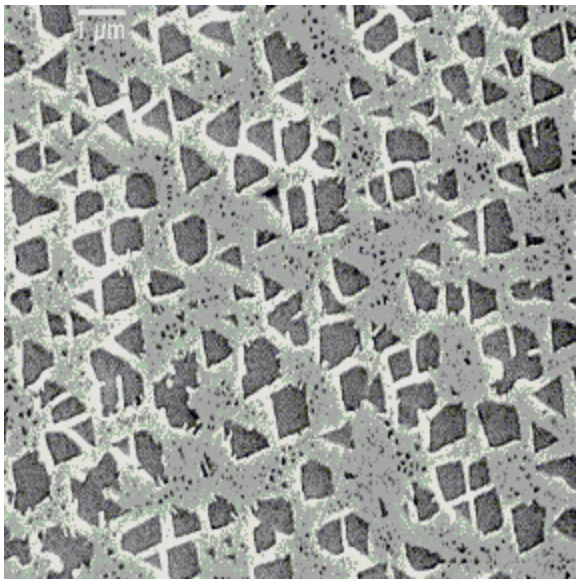

Figure 4 As-received microstructure of g ¢ precipitated IN738LC alloy showing duplex precipitate size distribution.

The cutting machine employed to obtain thin slices was the STRUERS brand, ACCUTOM – 5 model. An aluminum oxide cut-off wheel, STRUERS 456 CA (useable to maximum operational speed of 6300 rpm) was used. The speed and feed parameters adopted after several trial operations are given in **Table 2**.

Table 2: Speed and Feed Parameters for Cutting Samples from IN738LC Rods.

Operational Speed	3000 rpm
Feed	0.08 mm/sec
Force	Low
Coolant	STRUERS coolant (1 part in 33 parts of water)

Small pieces of the alloy IN738LC, about 4 mm thick and 6 mm edge length, were cut from the circular discs and then cleaned. The specimens were then individually wrapped in a stainless steel foil and sealed in silica tubes in vacuum. The stainless steel wrapping was to protect the specimens from contamination while heating in the silica tubes and to protect them from oxidation, if any. Solution treatment given to the

specimens were according to the following scheme. The alloy was heated to 1200 °C for 4 hours, to dissolve the solute atoms in the matrix crystal structure. The tubes, each containing four to six samples, were quenched in cold water and then reheated at 1120 °C for 24 hours resulting in a coarse (of size 700 nm) precipitate microstructure. The temperature was then raised to 1140 °C and the coarse precipitates were allowed to dissolve partially into the matrix. Water quenching the capsules after 6 hours at 1140 °C yielded the fine cooling precipitates resulting in the starting γ' precipitate duplex size distribution **[35]**.

Heat treatment is a procedure of heating the samples to different temperatures for different time periods and subsequently cooling to room temperature using specific cooling modes. They can vary from quenching in:

a) Iced salt water,
b) Water Quenching (WQ),
c) Air cooling (AC),
d) Accelerated air cooling (AAC), and
e) Furnace cooling (FC).

The heat treatment schedules (annealing) chosen in this study are indicated in **Table 3**.

After the above given solution treatment and attainment of the initial duplex size γ' precipitate microstructure, the capsules were broken and each specimen was resealed individually in a separate silica tube. The annealing consisted of reheating the samples under similar conditions (wrapped in stainless steel foils and sealed under vacuum) to different time periods. They were annealed at 800, 850, 900, 980, 1040 and 1100 °C for periods of 1, 3, 7, 13, 25, 50, and 100 hours. Six to eight capsules, each carrying one

sample, were put in the furnace at one of the chosen temperatures and heated for the different lengths of time given above.

Table 3: Heat Treatment Schedule for IN738LC with the Initial Duplex Size Precipitate Microstructure (Average Precipitate Size Data is also Included Wherever They Were Determined)

		Precipitate Sizes, μm						
Annealing Temp., ^{o}C	**Annealing Time, hr**	**1**	**3**	**7**	**13**	**25**	**50**	**100**
800		X				X	X	
	Fine	0.06				0.12		
	Coarse	0.31				0.38		
850						X		
	Fine					0.21		
	Coarse					0.48		
900			X		X	X	X	
	Fine					0.28		
	Coarse					0.55		
980		X	X	X	X	X	X	X
	Fine					0.37		
	Coarse					0.64		
1040		X	X	X	X	X	X	
	Fine	0.21	0.25	0.3	0.35	0.44	0.55	
	Coarse	0.48	0.525	0.58	0.64	0.69	0.73	
1100		X	X	X	X	X	X	X
	Fine	0.3	0.355	0.390	0.440	0.520	0.625	0.84
	Coarse	0.56	0.6	0.650	0.70	0.736	0.775	0.84

Only selected times among those given were adopted at different temperatures used and these are denoted by X in **Table 3**. The samples were individually removed after the specified time periods at the given temperatures and quenched in cold water. Cold water quenching was to retain the precipitate sizes in the microstructure after the given reheating.

It has been observed from the grain size data for the duplex size precipitate specimens after annealing at 1100 °C for different holding times that the fine precipitates grow rapidly to the same size as the coarse precipitates and reach an unimodal, single size precipitate distribution in the matrix. After 100 hours of ageing time, the average size of such single size unimodal particles is of the order of 840 nm, see **Table 3**.

In order to determine the maximum size possible for the coarsening precipitates, the independent samples were annealed at 1100 °C in vacuum under similar conditions for longer than 100 hours, up to 400 hours. The precipitates were seen to grow further and align up in long rafts in different directions. Coarsening of the rafts was also observed along with several solitary formations of large islands of precipitates. The formation of rafts under zero applied stress and subsequent coarsening is treated later in the analysis and discussion section of this thesis.

SEM micrograph of the specimen aged for 200 hours showed a very interesting phenomenon. The coarsened rafts and the large islands developed were seen to break up into several small fragments along the <111> directions. It appeared that dissolution of these fragments into the matrix occurred subsequently. A region of precipitate-depleted zone was also observed surrounding the breaking up rafts and coarse particles. Subsequent quenching to room temperature could have formed the fine cooling precipitates seen in the microstructure. Alternatively they could have been reformed at 1100 ^{o}C itself in regions where the coarse precipitates have completely broken down and dissolved. In order to establish, if these fine precipitates formed re-grow to the transient size again and this process repeats itself, in a cyclic manner, nine additional initial duplex precipitate specimens were annealed for various time periods from 150 hours to 350

hours. Specimens were withdrawn at intervals of 25 hours in this time span and water quenched. It was observed that the precipitates grew to maximum sizes, which peaked first at around 200 and then again at 300 hours, followed by subsequent breakdowns of the coarsest precipitates. Thus, it appeared that two growth and splitting cycles have been established. However, to look more closely into this phenomenon more specimens were felt to be needed and more initial duplex specimens were annealed at 1100 °C from 175 hours to 400 hours at intervals of approximately 12 hours. These are currently under study.

For precipitate microstructure studies, the samples were ground using grinding paper with coarse 120 to fine 600 ASTM grit sizes and polished on rotating wheels with fine alumina powder of size down to 0.05 micron. After cleaning, they were etched with a solution of composition 33 % HNO_3 + 33 % acetic acid + 33 % H_2O + 1 % HF (vol.%). Matrix grain morphology was revealed by etching with a solution of composition: 50 ml HCL + 50 ml H_2O_2 + 10 g Cu_2SO_4. A JEOL 840A Scanning Electron Microscope, equipped with an ultra-thin window EDS, was used to characterize the size and morphology of the γ' precipitates.

Microstructures were digitally recorded using a Macintosh Quadra data acquisition and control system and analyzed for precipitate grain size later. Photomicrographs were recorded at 1000, 2500, 8000 and 16000X. For precipitate size analysis, magnification of the micrographs reproduced was maintained the same in all cases at 8000 X (8 kX; 8 mm in precipitate photomicrographs = 1 μm) to facilitate direct comparison of precipitate sizes in different microstructures.

Precipitate size measurements were undertaken on the SEM photomicrographs. Reported precipitate sizes were obtained after measuring sizes of about 100 fine precipitates and as many medium size coarse precipitates as possible (usually about 25). The measurements were obtained manually by measuring the lengths along several diagonals and averaging those for each case. The average particle equivalent equimaxed sizes given in **Table 3** were then obtained for both the fine and coarse precipitates by using statistical analysis of the data collected. Precipitates in selected microstructures were also analyzed for composition using the Energy Dispersive Spectrometer (EDS) attached to the SEM.

Chapter 3. Results and Discussion – Part A

3.1 Microstructure Development and Characterization

Chemical composition of the γ′ precipitates in the superalloy IN738LC has been analyzed earlier **[35]** and its structure has been shown to be of the $L1_2$ type using X-ray diffraction. The volume fraction of the γ′ precipitate was determined to be 40-43 % in the FC condition and much lower, of the order of 23 % at 1120 ^{o}C/WQ and 30 % at 1050 – 1090 ^{o}C/WQ **[35]**, analogous to the values given in the literature.

3.2 Microstructure Modifications in the Duplex Precipitate Alloy at 800, 850, 900 and 980 ^{o}C for Different Holding Times

After solution treatment and initial ageing the starting microstructure had a duplex (bimodal) γ′ precipitate morphology, where the fine particles were of the order of 60 nm and the medium coarse particles were of the order of 300 nm in size. This is analogous to the specimen morphology at 800 ^{o}C after 15 mins, induction ageing **[20]**. Annealing the initial duplex size precipitate specimen at 800 ^{o}C/WQ for 25 hours and water quenching, **Figure 5 (a)**, showed the fine precipitates to become coarser, to about 120 nm, and the growth of the medium precipitates to 380 nm, see **Table 3**. Further growth of the fine and medium coarse precipitates could be observed when the specimens were aged for 50 hours, **Figure 5 (b)**.

Similar coarsening of the fine precipitates as well as further slow coarsening of the medium coarse precipitates were observed at 850, 900 and 980 ^{o}C. The sizes of the duplex (both primary and the cooling) precipitates are detailed in **Table 3** as function of temperature for different holding times. The SEM photomicrographs are included in **Figure 6** (850 ^{o}C, 25 hours/WQ), **Figure 7 (a), (b), (c), (d)** (900 ^{o}C, 3, 13, 25 and

50 hours/WQ), **Figure 8 (a), (b), (c), (d), (e), (f) and (g)** (980 ^{o}C, 1, 3, 7, 13, 25, 50 and 100 hours/WQ).

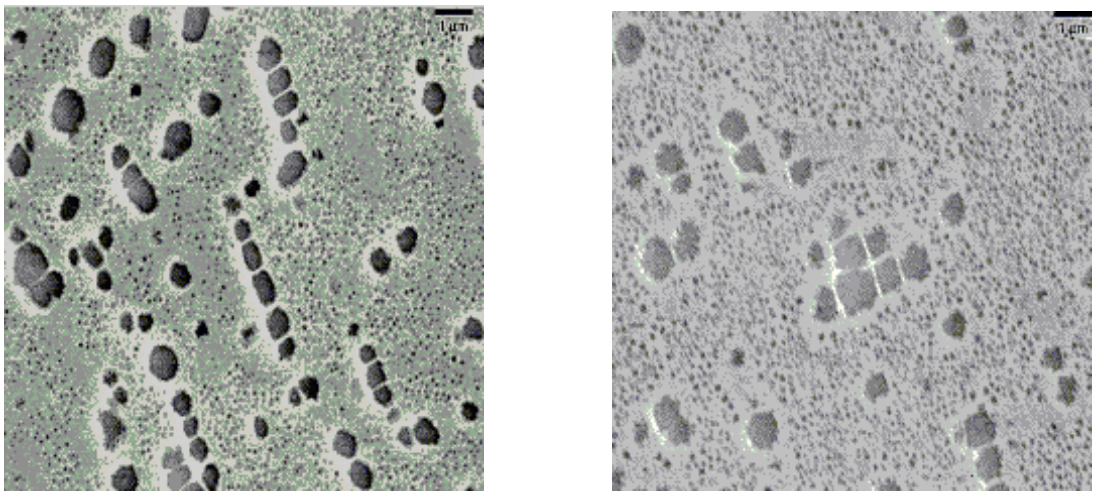

(a) **(b)**

Figure 5: Microstructures obtained subsequent to coarsening of fine and medium coarse precipitates after annealing at 800 ^{o}C for different holding times 't' and water quenching: (a) t = 25 h; (b) t = 50 h.

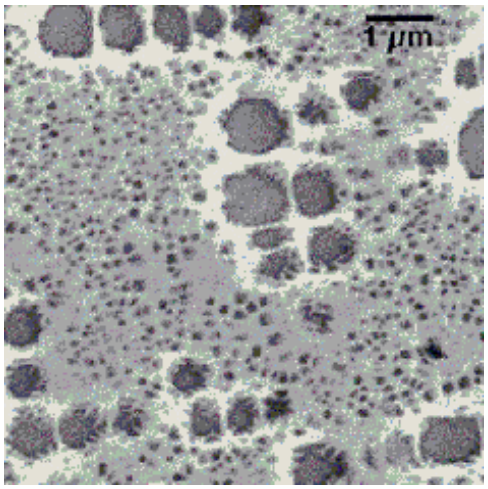

Figure 6: Microstructure after annealing at 850 ^{o}C for 25 h and water quenching

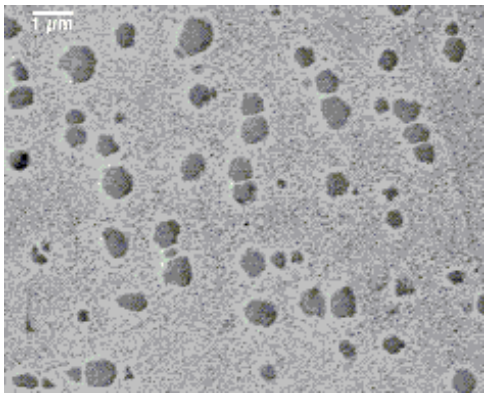

(a)

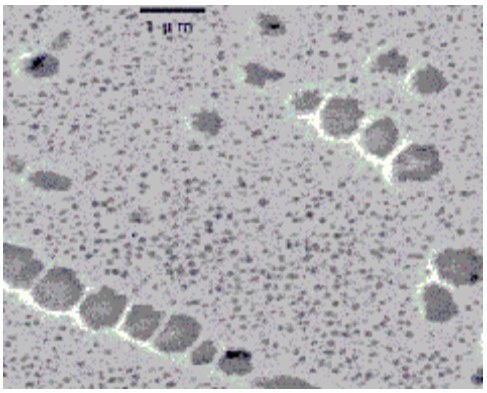

(b)

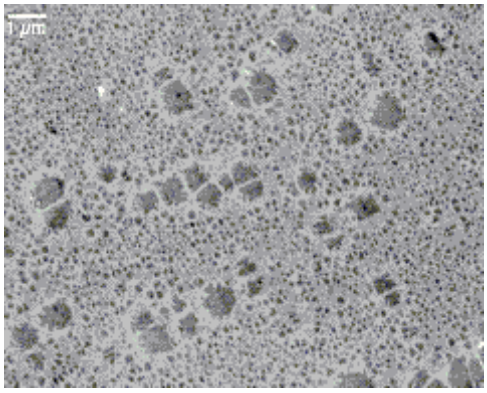

(c)

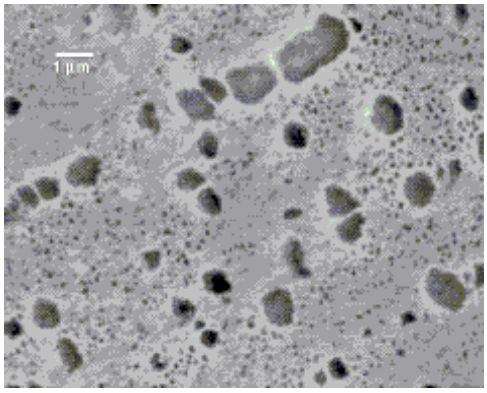

(d)

Figure 7: Microstructures after annealing at 900 ^{o}C for different times ‘t’ and water quenching: (a) t = 3 h; (b) t = 13 h; (c) t = 25 h; (d) t = 50 h.

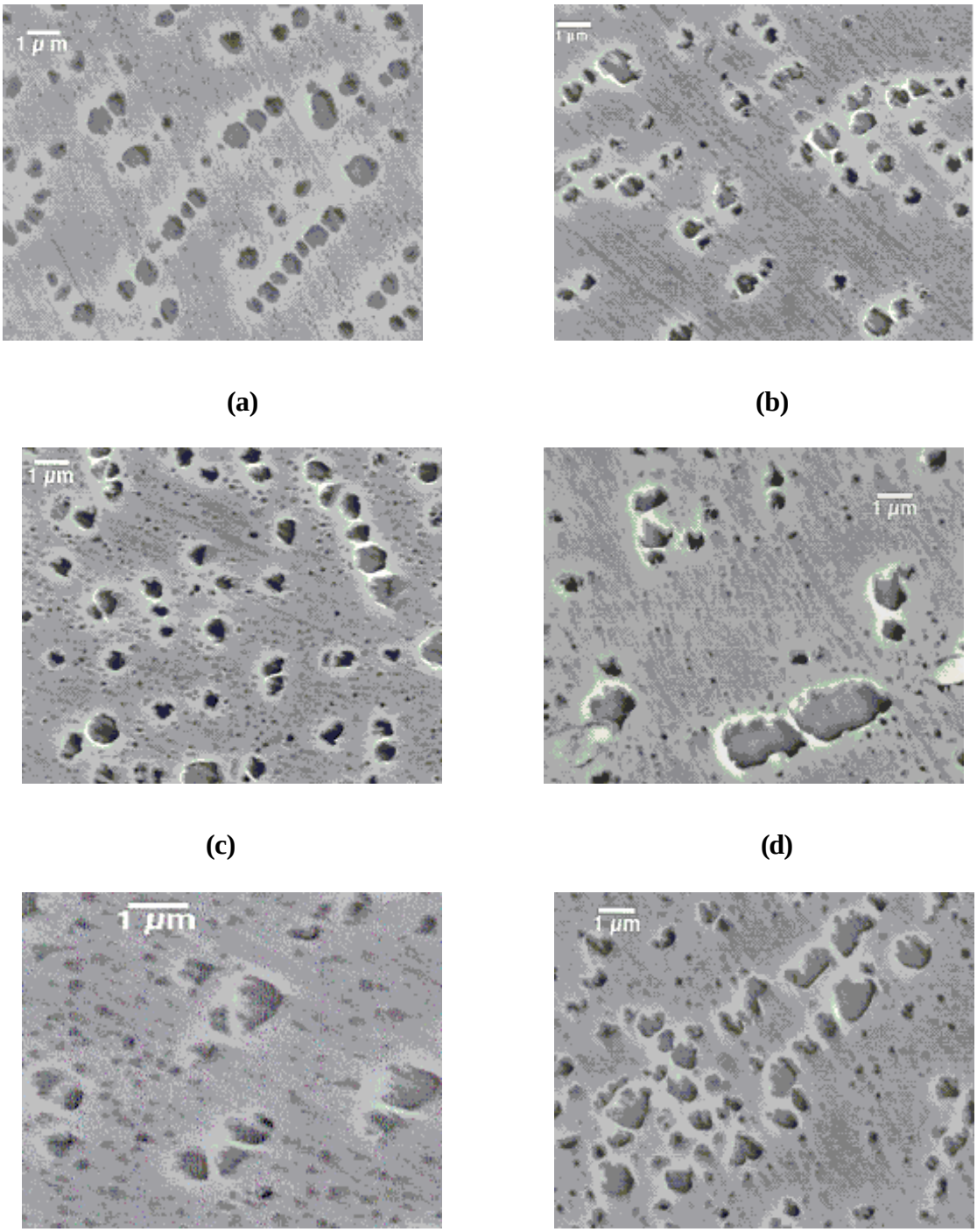

Figure 8: Microstructures after annealing at 980 ^{o}C for different times 't' and water quenching: (a) t = 1 h; (b) t = 3 h; (c) t = 7 h; (d) t = 13 h; (e) t = 25 h; (f) t = 50 h; (g) t = 100 h.

(Figure continued..)

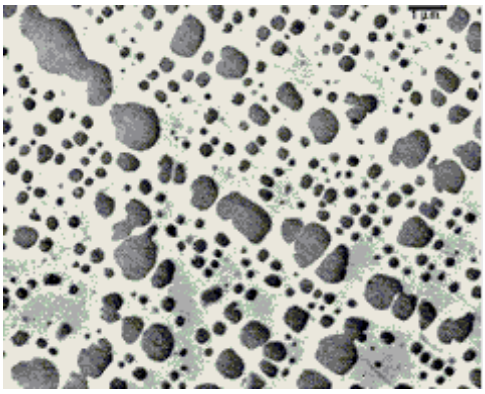

(g)

3.3 Microstructure Evolution at 1040 and 1100 ^{o}C for Different Holding Times

Both the fine and medium size γ' precipitates grew with time at a given temperature (e.g. 1040 ^{o}C). **Figure 9 (a), (b), (c), (d), (e) and (f)** show the microstructures obtained after annealing for various times at 1040 ^{o}C and **Figure 10 (a), (b), (c), (d), (e), (f) and (g)** for various times at 1100 ^{o}C. Precipitate shapes and sizes obtained after 25 hour annealing at the different temperatures used are shown in **Figure 11**. It is seen that the growth is slow at lower temperatures, whereas the growth rate is noticeably high at 1040 and 1100 ^{o}C, as can be expected. The fine precipitates are found not only to join with each other and coarsen, they also merge with the adjacent medium size precipitates coarsening them further **[17, 19, 27, 29-32]**. The fine precipitates gradually coarsen to the size of the growing medium size precipitates and after a certain time a single coarse size is realized. Thus, single size coarse precipitates are found after 100 hours of treatment at 1100 ^{o}C. It is thereby established that the duplex sized precipitates each grow continuously and ultimately become single-sized coarse precipitates.

Treating the fine-precipitate-containing alloy at 1120 ^{o}C for longer times showed earlier that the precipitates would grow to a maximum size of about 700 nm and then begin to dissolve partially even at 1120 ^{o}C. (1130 to 1150 ^{o}C is judged to be the normal precipitate partial dissolution and duplex size precipitate formation range). Similar coarsening and dissolution could occur at 1100 ^{o}C after a much longer time. This is discussed further in the next chapter of the thesis.

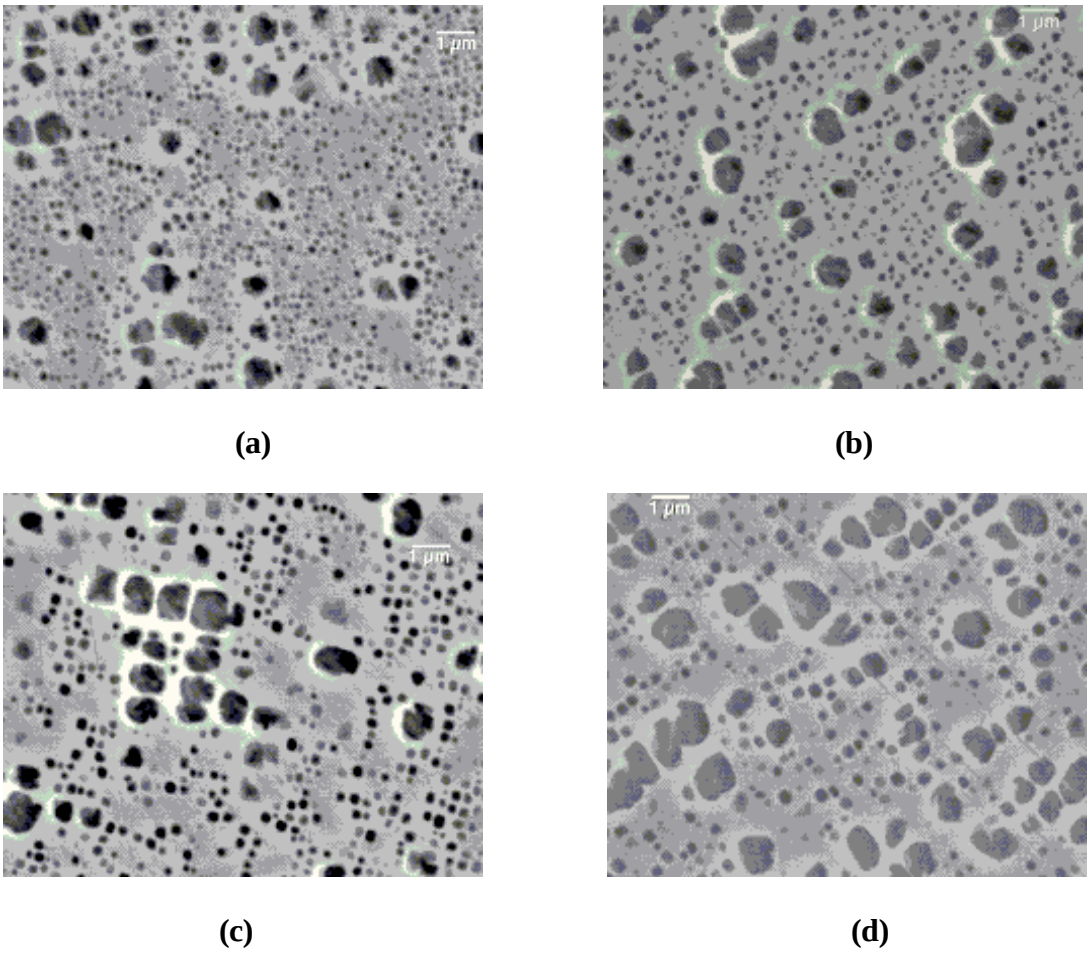

(a) **(b)**

(c) **(d)**

Figure 9: Microstructures after annealing at 1040 ^{o}C for different times 't' and water quenching: (a) t = 1 h; (b) t = 3 h; (c) t = 7 h; (d) t = 13 h; (e) t = 25 h;(f) t = 50 h.

(Figure continued..)

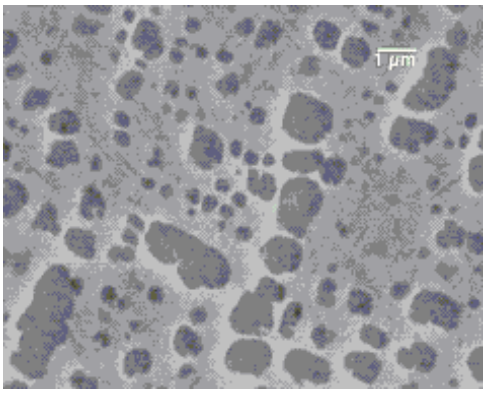

(e)

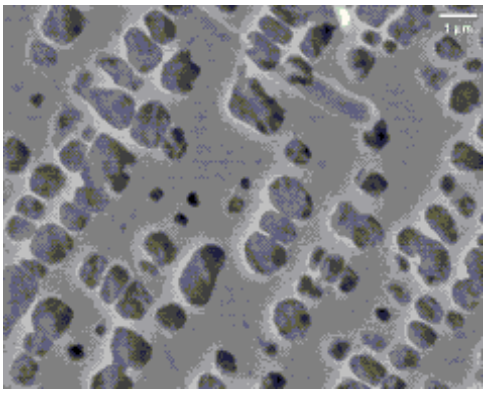

(f)

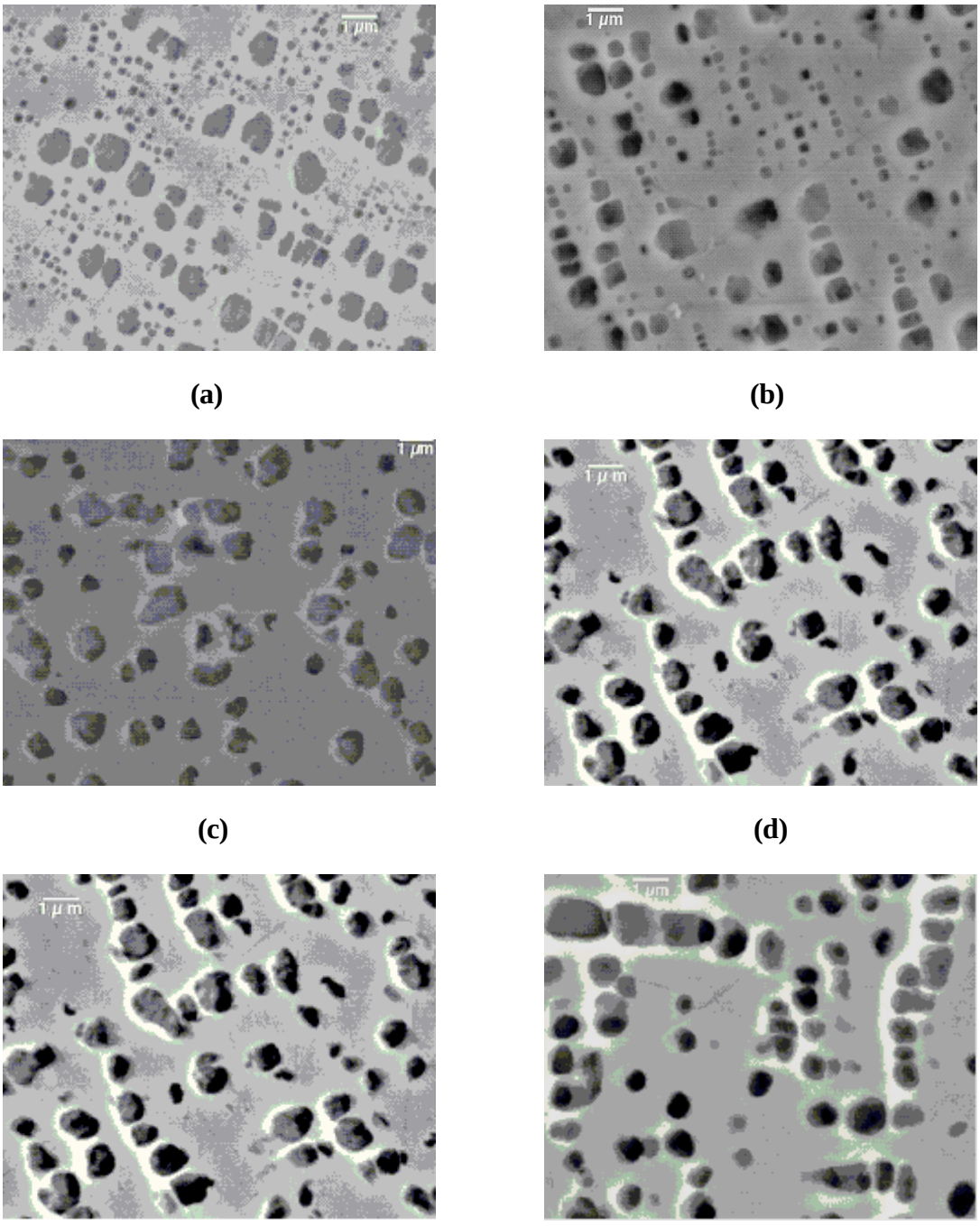

Figure 10: Microstructures after annealing at 1100 ^{o}C for different times 't' and water quenching: (a) t = 1 h; (b) t = 3 h; (c) t = 7 h; (d) t = 13 h; (e) t = 25 h; (f) t = 50 h; (g) t = 100 h.

(Figure continued..)

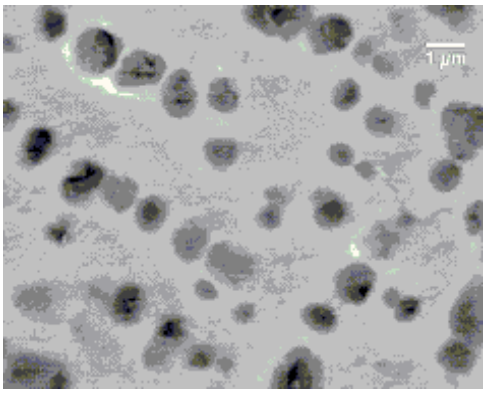

(g)

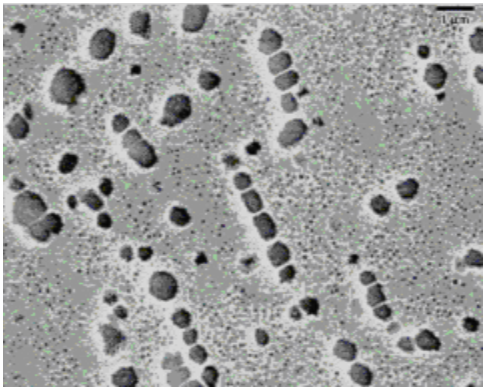

(a)

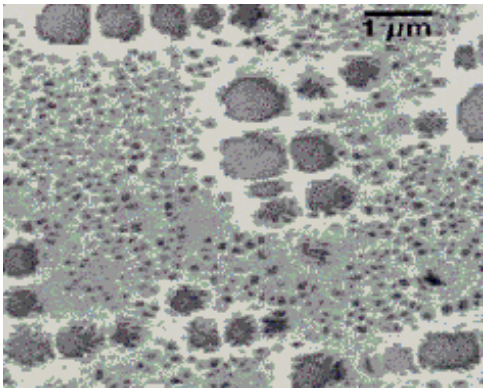

(b)

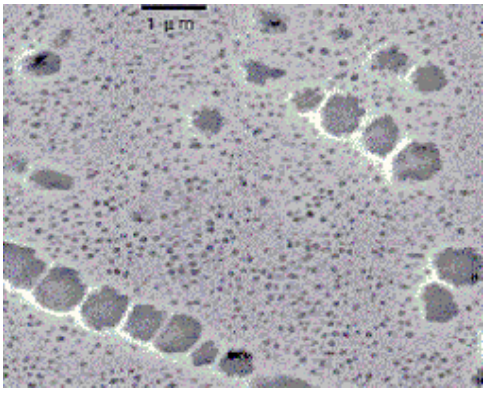

(c)

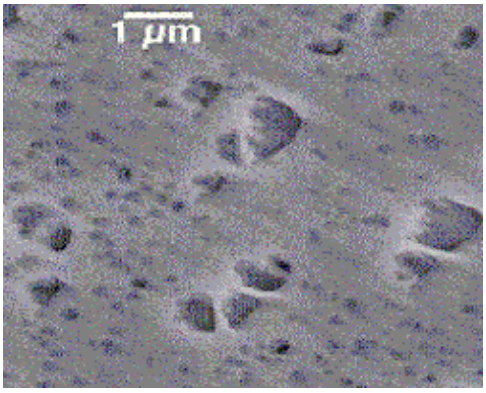

(d)

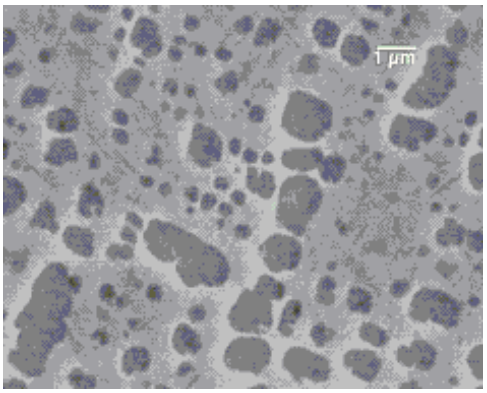

(e)

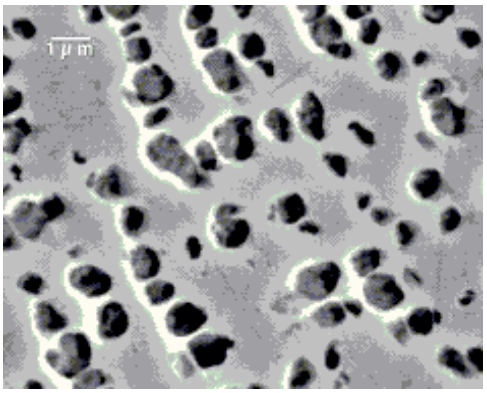

(f)

Figure 11: Microstructures obtained after 25 h annealing at different temperatures and water quenching: (a) 800 ^{o}C; (b) 850 ^{o}C; (c) 900 ^{o}C; (d) 980 ^{o}C; (e) 1040 ^{o}C; (f) 1100 ^{o}C.

Chapter 4. Results and Discussion – Part B

4.1 Precipitate Growth Features in the Duplex Size g ¢ Distribution in the Superalloy IN738LC

Two different growth mechanisms have been observed for the coarsening of the γ' precipitates. Precipitate growth by the Ostwald ripening process **[78]** and agglomeration of fine particles with each other and with the coarse ones, contributing to coarsening by the precipitate agglomeration mechanism (PAM), proposed earlier **[77]**. Analogous predictions in different other proposed models **[19, 27, 29-32]**, were found in the microstructures of a few annealed samples at the initial stages, **Figure 12**. It is clear that the coarse particles attract the nearby fine particles leading to their further coarsening by the agglomeration process, simultaneously denuding the zone around them of the fine ones. From the sizes of precipitates obtained from different microstructures, the molar activation energy for the growth process for both the fine and the coarse precipitates were calculated assuming the LSW diffusion mechanism using the formula **[79]**:

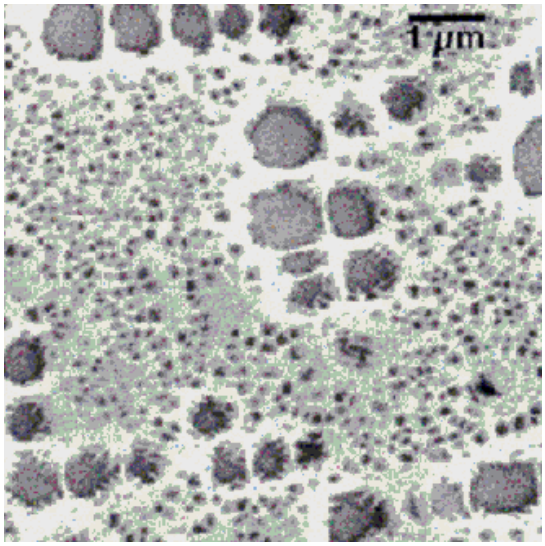

Figure 12: Coarsening by particle agglomeration

$$d_t^n - d_0^n = Kt \text{ where } K = K_0 \exp\left(-\frac{Q}{RT}\right) \text{ ....(7)}$$

wherein d_0 is the initial size of the particle to start with at t = 0, d_t is the size after a heating time of 't' at the temperature T, n is the growth exponent generally (assumed to be 3) and Q is the molar activation energy for the growth process **[74]**. It is not certain, however, whether this equation, originally given by Wagner **[14]** and Lifshitz and Slyazov **[13]**, would still be valid for the precipitate growth by the particle agglomeration mechanism. It can be expected to prevail if the particle motion is controlled in some way by the diffusion of atoms in the matrix. Here, an attempt is made to analyze the precipitate size data obtained using this LSW model modeled for precipitate growth.

Average size data obtained are plotted in **Figure 13** for the 25-hour treatment at different temperatures and in **Figure 14 (a) and (b)** for different times at 1040 ^oC and 1100 ^oC, respectively. The data in **Figure 13 and Table 3** are replotted as ln(d) vs. 1/T plots in **Figure 15**. These plots were found to have five different linear segments with slightly different slopes in the temperature ranges between adjacent temperatures, see **Table 3**. From the slopes of these linear segments the Q values were calculated. Each Q value was then taken to prevail in the corresponding temperature range and was plotted in a separate figure, **Figure 16**, as Q vs. mean T plots. The mean temperature was chosen, since there are two slopes of adjacent temperature ranges and hence two different Q values for the end temperatures of each range. Corresponding to these mean temperatures the 'd' values can be calculated from the slope equations and using this data corresponding Q vs. 'd' plots were generated and plotted in **Figure 18** (plots for 25h treatment at different temperatures).

From the data of precipitate sizes at the two temperatures 1040 and 1100 ^{o}C for different times (given in **Figure 14**), activation energy Q for the precipitate growth process could also be calculated from the two values of the size data of the coarse or fine precipitates corresponding to the two temperatures for a specific time. This Q value was taken to prevail in the temperature range 1040-1100 ^{o}C and, for similar reasons as stated earlier, was taken corresponding to the mean temperature 1070 ^{o}C and the specific holding time. **Figure 17** gives the plots of Q vs. holding time 't' for the fine and coarse particles corresponding to the mean temperature 1070 ^{o}C. Taking the average of the precipitate sizes at the two temperatures corresponding to a given holding time as the size of the precipitate at the mean temperature for the same holding time, the above Q vs. 't' plots could be converted to Q vs. 'd' plots. These plots are also included in **Figure 18** (plots for mean temperature 1070 ^{o}C for different times).

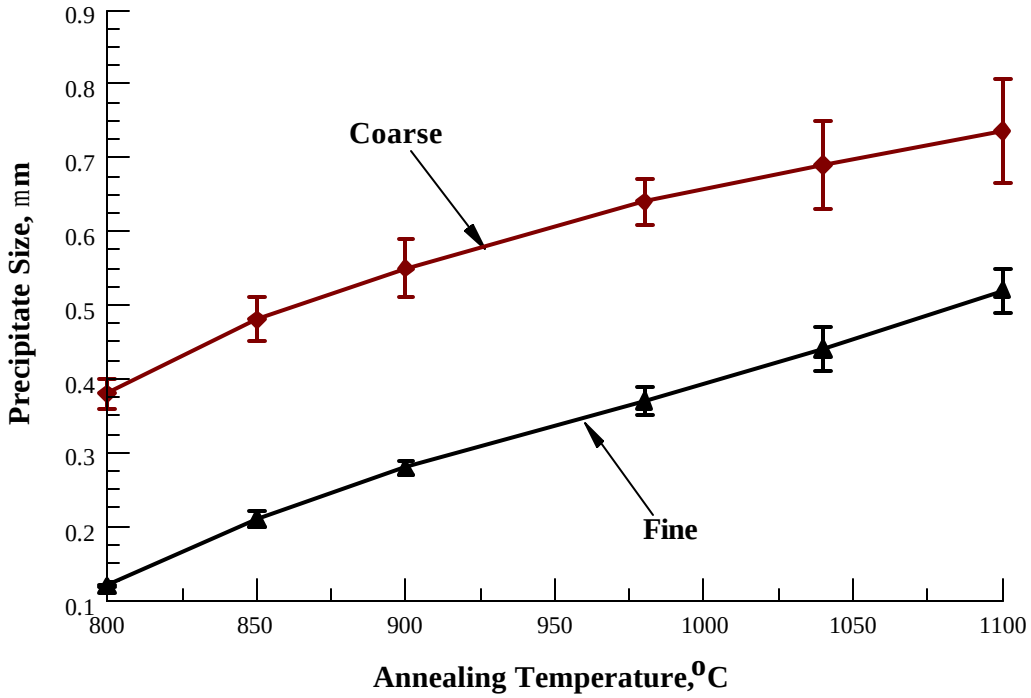

Figure 13 Plots of precipitate size data after 25 hour annealing treatment at different temperatures.

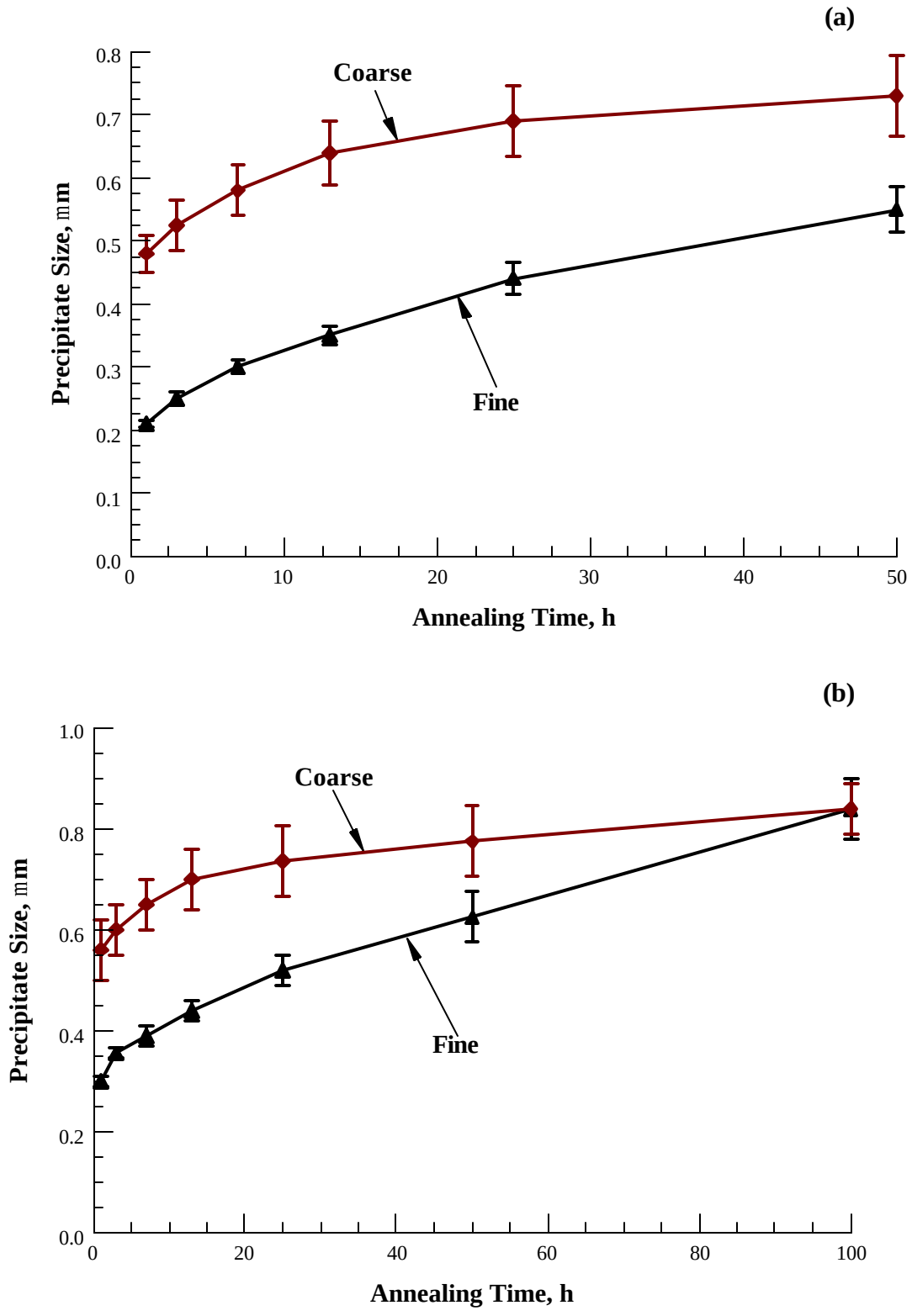

Figure 14 Plots of precipitate size data for different annealing times in the range 1 to 100 h at (a) 1040 °C (b) 1100 °C.

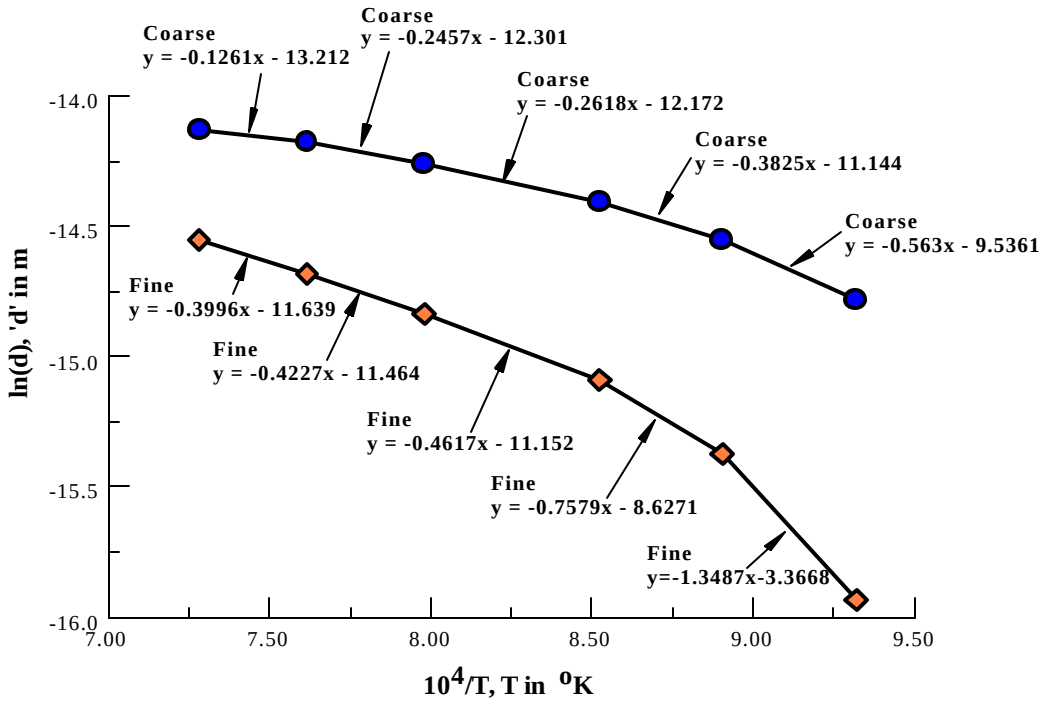

Figure 15 Plots of ln(d) vs. 1/T (T = 1073 -1373 °K) for coarsening of fine and coarse precipitates after 25 h annealing time.

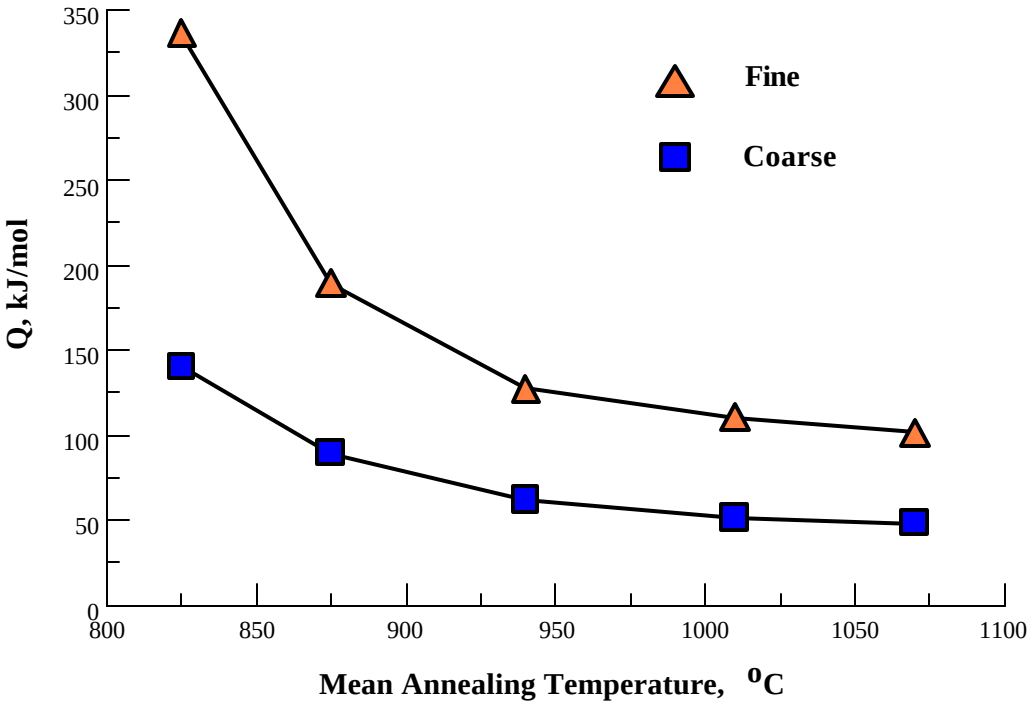

Figure 16 Activation energy 'Q' for precipitate coarsening of fine and coarse particles in the duplex size distribution plotted against average temperature in the range between adjacent temperatures (from 25 h annealing data).

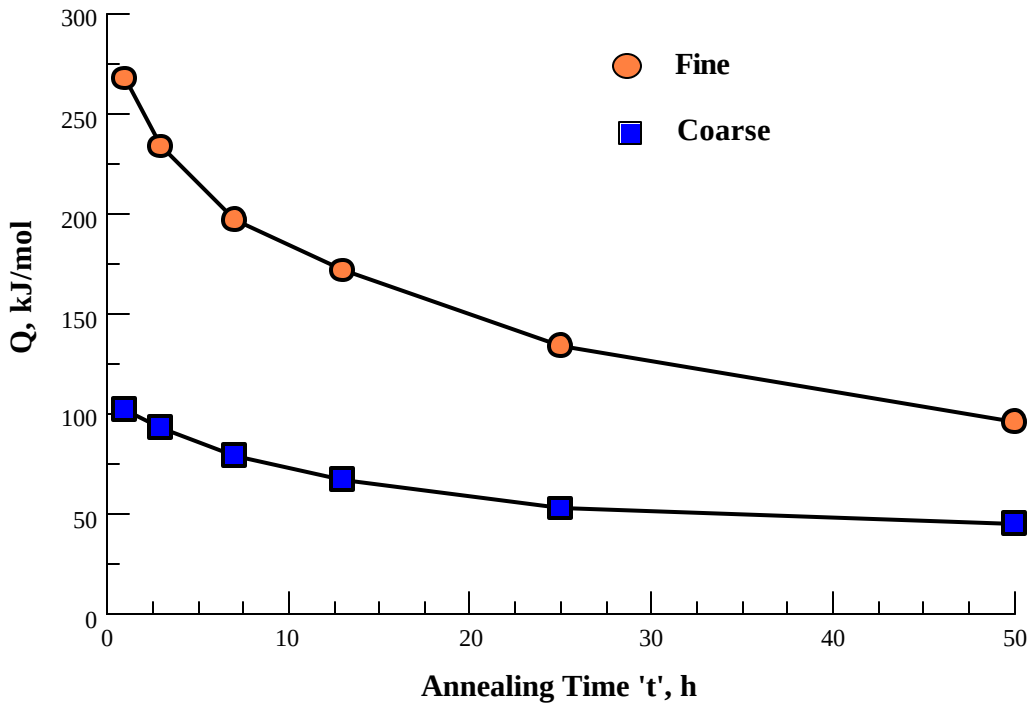

Figure 17 Activation energy 'Q' for precipitate coarsening of fine and coarse particles in duplex size distribution, plotted against annealing time 't' (calculated from the size data for specific 't's at 1040 and 1100 ^{o}C and taken to represent the 'Q' values for the mean temperature 1070 ^{o}C).

The above plots show that the activation energy is not a constant in the temperature range 800 to 1100 ^{o}C, but varies continuously. Also the activation energies for the growth of coarse precipitates are smaller than the analogous values for the growth of fine precipitates. It is observed that there is a decrease in the activation energy for the growth of the coarse or fine particles for 25 h annealing time with an increase in temperature. The activation energy for the growth also is found to decrease with increasing size of the precipitate with increasing holding time at a given temperature, 1070 °C, for both the fine and coarse precipitates. It is noticed that both sets of data show analogous drop in Q with increasing 'd' and the offset between the plots of the two different sets of data becomes progressively minimal as the size of the particles increases.

This can be attributed to slight inaccuracy in the estimation of the average size of fine particles and to somewhat better accuracy in the determination of the size of the coarse particles.

The above results clearly indicate that the activation energy for the growth of precipitate particles in the duplex size range is not a constant, but depends on the size of the particles. It is clear that it decreases with increasing size of the particles in the duplex structure, which would imply that the coarser particles grow more easily in the duplex structure, needing less activation energy than for the finer particles.

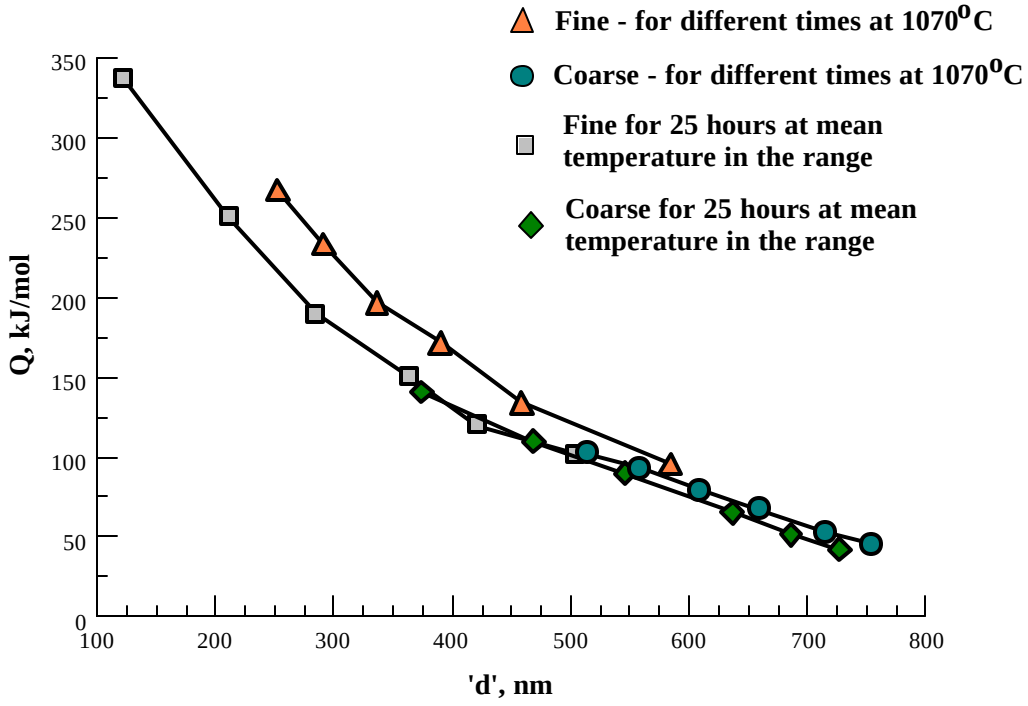

Figure 18 Combined figure showing all data of activation energy 'Q' for precipitate coarsening of fine and coarse particles in duplex size distribution vs. precipitate size 'd'. 'd' is calculated from the slope equations in Figure 15 for the mean temperatures of the various ranges (for 25 hours annealing) and from particle sizes for various times at 1040 and 1100 °C in Figure 14 (for the mean temperature 1070 °C).

This can be attributed to the larger attractive force (enunciated in the PAM model **[77]**) the coarser particles would exert on the finer particles, while the corresponding agglomerating force would be weaker for the finer particles. The larger attractive force apparently makes it easier for the fine particles to move through the matrix and this leads to a reduction in the activation energy needed for particle agglomeration and the resultant size increase. As the attractive force is stated to increase progressively with the increase in size of particles, progressively there is also an appropriate decrease in the activation energy needed to consolidate the adjacent particles and contribute to the size increase of the coarser particles. Thus, the results obtained in this work reinforce the particle agglomeration mechanism enunciated earlier for the growth of particles in the duplex size precipitate microstructure **[77]**.

4.2 Precipitate Growth Mechanisms and Kinetics in the Superalloy IN738LC

IN738LC shows the duplex size γ' microstructure following the partial dissolution of coarse precipitates starting from the coarsest ones **[35]** or during the growth from fine ones **[34]** in the range 1130 – 1150 ^{o}C and water quenching. Also when quenched from the temperature of 1120 ^{o}C after prolonged annealing the alloy shows a duplex size γ' microstructure **[77]**. When quenched from the temperature range 1160 – 1225 ^{o}C, the alloy has a fine precipitate microstructure of the 'cooling precipitate'**[77]**. The source for the formation of the fine precipitates (even in the case of the duplex (bimodal) morphology) is possibly the dissolution of some of the smaller newly grown precipitates, (cuboidal precipitates) **[77],** and corner dissolution of coarse cuboidal precipitates in the temperature range 1130-1150 ^{o}C **[77]**.

The morphological transformation of the precipitates from cuboidal to spheroidal can be attributed to the requirement of reduction in surface area for the coarse cuboidal precipitates. Normally a low interfacial energy between the precipitate and the matrix, compared to other transformation energies, allows for precipitate growth through solute pick up from the solid solution matrix (Ostwald ripening). Because of the fact that materials thermodynamically prefer the lowest possible state of total free energy, it appears that the coarse γ' precipitates dissolve at higher than a critical temperature and / or size leading to a possible reduction of interfacial energy as well as strain energy associated with coherency and re-precipitate as many very fine ones upon quenching. This enables the accommodation of a larger surface area. However overall free energy is kept approximately unchanged, corresponding to that at a given temperature.

The growth of a few precipitates by merging can also be explained on the basis of the need for reduction in total surface area and to prevent an increase in the overall surface energy. Smaller particles migrate as a whole to the nearby coarse particles and join with them, or coalesce with nearby fine ones as well, at relatively high temperatures. This points to the fact that the matrix is considerably softened to enable such migration. Also an attractive force between such agglomerating particles due to elastic strain fields can be postulated **[77]**.

Precipitates generally coarsen by picking up solute atoms from the matrix driven by the atomic diffusion process. Coarsening can also occur by particle agglomeration mechanism (PAM) **[77]**, also in line with analogous models in other works **[19, 27, 29-32]**, different from the Ostwald ripening process of conventional solute atom diffusion process in the matrix. This has been observed in the case of this superalloy

IN738LC also. The particle migration and agglomeration process can still be considered as activated by the inter-diffusion of atoms at the interface leading to its migration in the direction of its greatest pull from the attractive force, activating the migration of the precipitate as a whole in the matrix medium. The precipitate coalescence takes place at a nearly constant volume fraction in the temperature range 650-1130^{o}C.

The first hypothesis on the precipitate movement in the matrix as a whole for the agglomeration purpose was made by R. D. Doherty **[31]**. He indicated that the precipitates could move toward each other and join by the removal of elastically strained matrix. Voorhees and Johnson **[49]** did the first theoretical analysis of the particle migration in the matrix, driven by elastic stresses. Their work extended to developing the formula for the growth rate and migration velocity of the mass center of precipitates on the basis of the elastic energies. There are other similar and analogous models in other works **[19, 27, 29, 30, 32]**. The general finding is that the sign of the misfit and applied stresses, the ratio of the elastic properties of the matrix and the precipitate phases, and the interfacial energy significantly affect the precipitate morphology evolution. Some of the findings indicate an inverse coarsening, where smaller precipitates may grow at the expense of the larger ones, due to the elastic interactions between the precipitates, quite the opposite of Ostwald ripening.

In the particle agglomeration model (PAM) **[77]**, the requirement for more energy for the coalescence process has been clearly explained by distinguishing between the processes for the growth, one via the dissolution and atomic diffusion and the other via coalescence. Based on the observations made **[77]**, PAM postulates that the consolidation of the adjacent particles by particle motion is due to an attractive force F_A

exerted by the particles on one another. This attractive force is said to be developed by the need to reduce the overall surface interfacial energy of the particles as well as the elastic strain energy of the matrix at a given temperature, which is determined by the total surface area and volume or mass of the particle.

Chapter 5. Results and Discussion

5.1 The Particle Break-up Mechanism (PBM) of the Strengthening g ¢ Precipitates in the Duplex Size Distribution on Annealing at 1100 ^{O}C for 200 Hours in the Superalloy IN738LC.

After the solution treatment and the initial ageing treatments as described in section 2.2, the initial starting microstructure had a duplex (bimodal) γ' precipitate morphology, where the fine particles were of the order of 60 nm and the medium coarse particles were of the order of 300 nm in size. Annealing the specimens at 1100 ^{o}C for 100 hours and water quenching showed the fine precipitates becoming coarser and reaching the size of the slowly growing coarse precipitates, finally reaching a uniform coarse microstructure of 840 nm. To estimate the maximum size attainable by the coarsest precipitates, the alloy with the initial duplex size precipitate microstructure was further annealed for long time periods in the range 150 to 350 hours, withdrawing individual specimens at 25-hour intervals.

The precipitates were observed to coarsen further. Long raft patterns (particles joined along a line) were developed in different orientations along with formation of several distinctly large islands of agglomerated precipitates. The rafts were seen to coarsen along with further growth of the precipitate islands. An SEM photomicrograph of the specimen annealed for 200 hours at 1100 ^{o}C is shown in **Figure 19**. It shows a very interesting phenomenon. The coarsened rafts and the large islands developed are seen to break up into many fine precipitates in parallel arrays **Figure 19**. A region of precipitate depleted zone is also observed around the breaking up rafts and coarse particles. That the big and the coarse particles break-up into many fine particles of size equivalent to those of 'cooling precipitates' is obvious in the microstructure shown in **Figure 19**. Note that

all the coarse particles are breaking up. Looking at several such breaking particles, it is seen in many that the break-up is initiated at the surface along a line if the particle is big (of the order of ~ 2 μm in size), but when the particles become progressively thinner after such break-up the whole particle break up into many fine ones located along parallel lines. Two distinct directions of fine particle arrays inclined at ~ 120 ^{o} to each other, are noticed in the completely breaking particles situated at the lower left regions of the figure. This might imply that the particle break-up directions are along the <111> of the FCC lattice.

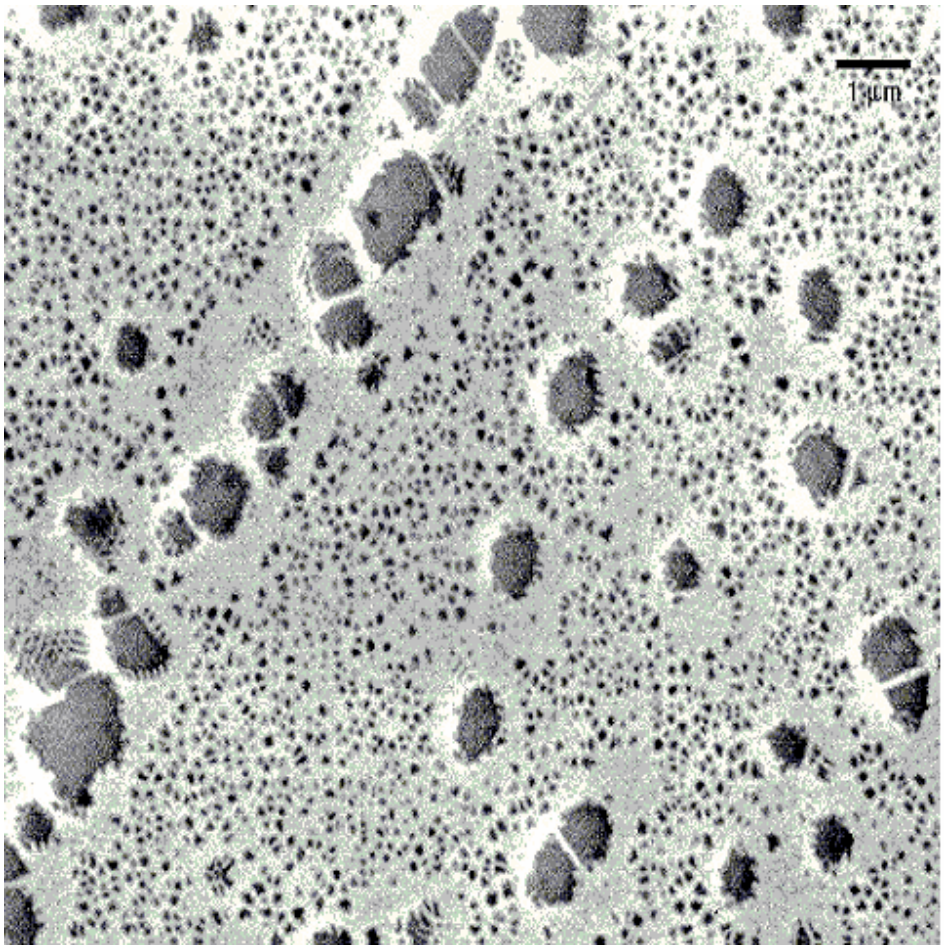

Figure 19 Microstructure after 200 hour annealing at 1100 ^{o}C. Particle break-up along a direction of a raft is clearly illustrated. Particles break-up into fine fragments along two directions, 120^{o} apart, indicative of breakdown along <111> directions.

It is also apparent that the fine particles so produced by the particle break-up process dissolve into the matrix and disappear. The denuded zone around the breaking coarse particles indicates that nucleation of cooling precipitates does not take place in this region. A repulsion force propelling the solutes in the matrix from the dissolving coarse precipitates can be postulated. In the rest of the area cooling precipitates are seen to have formed and evenly distributed in the matrix. This implies that the solute redistribution shall occur rather fast into the region where the coarsest particles have completely broken-up and dissolved, right after their complete disappearance through dissolution. The question now arises: If the coarsest particles disintegrate and dissolve into the matrix, do they reform as fine ones at the annealing temperature, grow again to the maximum size, break-up and whether this process occur in cycles.

5.2 g ¢ Precipitate Particle Elastic Strains and Interactions (Particle Break-up Mechanism (PBM))

A precipitate present in a solid matrix has an excess energy associated with it. This energy can be split into three parts **[80]**.

$$E = E1 + E2 + E3 \qquad (8)$$

where E1 is the elastic strain energy due to lattice mismatch between precipitate and matrix. E2 is the interfacial energy of the precipitate. The precipitate takes a particular shape so as to minimize E1 + E2. The energy E3, is the elastic interaction energy between the precipitates due to overlap of strain fields when the inter particle distance becomes small. Owing to this elastic interaction non-spherical γ' precipitates in γ/γ' superalloys become aligned along the <100> directions. This effect has been able to produce rafted structures in superalloys with improved high temperature creep

properties **[81]**. Kachaturyan, et al. **[82]** developed a theoretical analysis to model morphological changes occurring during the coarsening of cube shaped precipitates. This model implies that as particles grow beyond a critical size, they split into smaller particles due to the effects of elastic interaction, thus not permitting a continuous increase in the mean size with increase in ageing time beyond a certain limit. This leads to a possibility of stabilization of the microstructure. The splitting phenomenon is just the reverse of the coalescence in the sense that the splitting of precipitates leads to a discontinuous decrease in size. One of the arguments proposed for coalescence not taking place between two particles, which are very close to each, other but out of phase, is the necessity of forming an APB. If two particles have instantaneously coalesced and the size corresponds to the size at which the particle should split according to the splitting model, then it comes to the point whether there will be any coalescence in the first place.

Several investigations have been directed toward studying elastic interactions between solid particles in a solid matrix. Ardell, et al. **[83]** reported that there is a resistance to coalescence due to the presence of elastic interactions. They also state that the kinetics of coarsening remain unaffected by the presence of elastic strain fields. When the lattice mismatch in alloys is small, where the precipitates are spherical in shape, there is no appreciable alignment. Ardell has shown **[84]** that as the lattice mismatch increases the greater is the particle size found at a particular ageing temperature. Systemic experimental studies should throw light on the effect of elastic strains on coarsening as well as on break-up.

Chapter 6. Conclusions and Suggestions for Further Work in This Area

The following constitutes the salient conclusions from this research.

The activation energies for coarsening of the coarse precipitates are smaller than the analogous values for the growth of fine precipitates, in duplex size precipitate distribution.

The experimental results clearly indicate that the activation energy for the growth of the precipitate particles in the duplex size range is not a constant, but depends on the size of the particles.

There is a decrease in the activation energy for the growth of the coarse or fine particles for similar annealing time with an increase in temperature.

The activation energy for the growth also is found to decrease with increasing size of the precipitate with increasing holding time at a given temperature, 1040 °C, for both the fine and coarse precipitates.

The activation energy for coarsening in the duplex distribution seems to decrease with increasing size of the particles implying that the coarser particles grow more easily in the duplex structure, needing less activation energy than for the finer particles. This can be attributed to the larger attractive force (enunciated in the PAM model **[77]**). The coarser particles would exert on the finer particles, while the corresponding agglomerating force would be weaker for the finer particles.

The larger attractive force apparently makes it easier for the fine particles to move in the matrix towards the adjacent coarse particle and this leads to a reduction in the

activation energy needed for particle agglomeration and the resultant size increase. Since the attractive force increases with the increase in particle size, progressively less activation energy is needed to consolidate the adjacent particles and contribute to the size increase of the coarser particles as the particles grow. Thus, the results obtained here reinforce the particle agglomeration mechanism enunciated earlier for the growth of particles in the duplex size precipitate microstructure **[77].**

From our experimental results, in the duplex size precipitate distribution, after annealing beyond 100 hours at 1100 °C, after obtaining a unimodal, single size coarse precipitate microstructure, on further ageing, the precipitates were observed to coarsen more. Long raft patterns were developed in different but distinct orientations along with formation of several distinct formations of large islands of agglomerated precipitates. The rafts were seen to coarsen with further growth of the precipitate islands. At 200 hours of ageing, the coarsened rafts and the large islands developed were seen to break up from the corners into and fine precipitates line up in parallel arrays along two directions ~ 120^{o} apart, our results indicate that the break-up possibly occur along the octahedral <111> directions of the FCC $L1_2$ structure.

Based on the results obtained in this study, and in view of the industry requirements, modeling creep in the duplex microstructure is required to be delved into. The application and further refinement of the PAM model will be very important for predicting coalescence and coarsening mechanisms in different precipitate size distributions.

The effect of the growth and break up of the precipitates in the duplex size precipitate distribution on high temperature creep will be of enormous significance. This

brief outline lists only a few of the numerous research questions necessary to be studied in view of the practical application of the material at high temperatures in the industry and exemplifies the richness of the project.

References

1. M.J. Wahll, D.J. Maykuth and H.J. Hucek, “Handbook of superalloys” (Battelle Press, Columbus, 1979), pp.1.

2. D. Bettge, W. Osterle and J. Ziebs, Z. Metallkunde, 1995, Vol. 86(3), 190.

3. R.A. Ricks, A.J. Porter, and R.C. Ecob, Acta. Met., 1983, Vol. 31, 43-53.

4. A.V. Karg, D.E. Fornwalt and O.H. Kriege, J. Inst. Met., 1971, Vol. 99, 301.

5. N.F. Mott and F.R.N. Nabarro, Proc. Phy. Soc., 1940, Vol. 52, 86.

6. V. Munjal and A.J. Ardell, Acta Metall., 1975, Vol. 23, 513.

7. P.S. Kotval, Metallogr., 1969, Vol. 1, 251.

8. G.P. Sabol and R. Stickler, Phys. Status. Solidi., 1969, Vol. 35(11), 11.

9. R.F. Decker and C.T. Sims, “The Superalloys”, (Wiley, New York, 1979), pp.33.

10. A.K. Jena, M.C. Chaturvedi, Journal of Material Science, 1984, Vol. 19, 3121.

11. A. Ges, H. Palacio and R. Versaci, Journal of Materials Science, 1994, Vol. 29, 3572.

12. F. Shubert, “Phase Stability in High Temperature Alloys”, 1980, pp.119.

13. I. Lifshitz and V. Slyozov, Journal of Phys. Chem. Solids., 1961, Vol. 11, 35.

14. C. Wagner, Z. Elect., 1961, Vol. 65, 581.

15. H. F. Merick, “Precipitation in Ni-base Alloys”, ICSMA 1976, Vol. 1, pp. 61.

16. G.W. Greenwood, Acta Metall., 1956, Vol. 4, 243.

17. A.J. Ardell, Acta Metall., 1972, Vol. 20, 61.

18. A.J. Ardell and R.B. Nicholson, Journal of Phys. Chem. Solids. 1966, Vol. 27, 1793.

19. A.J. Ardell and D. Chellman, Acta Metall., 1974, Vol. 22, 577.

20. S.H. Razavi, S.H. Mirdamadi, J. Szpunar and H. Arabi, Journal of Material Science, 2002, Vol. 37, 1461.

21. C.S. Jayanath and Philip Nash, Journal of Materials Science, 1989, Vol. 24, 3041.

22. A.D. Brailsford and P. Wynblatt, Acta Metall., 1979, Vol. 27, 489.

23. P.W. Voorhees and M.E. Glicksmann, Acta Metall., 1984, Vol. 32, 2001.

24. P.W. Voorhees and M.E. Glicksmann, Acta Metall., 1984, Vol. 32, 2013.

25. J.A. Marqusee and J. Ross, J. Chem. Phys., 1980, Vol. 80, 536.

26. M. Tokuyama and M. Kawasaki, Physica., 1984, Vol. 123A, 386.

27. C.K.L. Davies, P. Nash and R.N. Stevens, Acta Metall., 1980, Vol. 28, 179.

28. C.K.L. Davies, P. Nash and R.N. Stevens, J. Mater. Sci., 1980, Vol. 15, 1521.

29. S.S. Kang and D.N. Yoon, Met. Trans., 1982, Vol. 13A, 1405.

30. S.S. Kang and D.N. Yoon, Met. Trans., 1981, Vol. 12A, 65.

31. R.D. Doherty, Metal. Sci, 1982, Vol. 16, 1.

32. P.K. Rastogi and A.J. Ardell, Acta Metall., 1971, Vol. 19, 321.

33. P.K. Footner and B.P. Richards, Journal of Material Science, 1982, Vol. 17, 2141.

34. E. Balikci, A. Raman, Journal of Material Science, 2000, Vol. 35, 3593.

35. E. Balikci, A. Raman, Metallurgical and Materials Transactions A, 1997, Vol. 28A, 1993.

36. D. Mukherji, F. Jiao, W. Chen and R.P. Wahi, Acta Metall., 1991, Vol. 39(7), 1515.

37. J. Li, R.P. Wahi, H. Chen, W. Chen and H. Wever, Z. Metallkunde, 1993, Vol. 84(4), 268.

38. J. Li and R.P. Wahi, Acta Metall., 1995, Vol. 43(2), 507.

39. Y. Wang, D. Mukherji, W. Chen, T. Kutter, R.P. Wahi and H. Wever, Z. Metallkunde, 1995, Vol. 86(5), 365.

40. D. Bettge, W. Osterle and J. Ziebs, Z. Metallkunde, 1995, Vol. 86(3), 190.

41. H. Chen, W. Chen, D. Mukherji, R.P. Wahi and H. Wever, Z. Metallkunde, 1995, Vol. 86(6), 423.

42. T. Malow, J. Zhu and R.P. Wahi, Z. Metallkunde, 1994, Vol. 85(1), 9.

43. C.G. Bieber, Suffern and J.J. Galka, United States Patent Office, No. 3459545, August 1969.

44. J.K. Tien and T. Caulfield: Superalloys, Supercomposites and Superceramics, Academic Press, Inc., NY, 1989, pp. 132.

45. L. Liu, F. Sommer and H. Z. Fu, Scripta Metall and Mater., 1994, Vol. 30, 587.

46. L. Liu, B.L.Zhen A. Banerji, W. Reif and F. Sommer, Scripta Metall and Mater., 1994, Vol. 30, 593.

47. C.G. Bieber and J. R. Mihalisin, Proc. Second International Conference on the Strength of Metal and Alloys, Pacific Grove, CA, 1970, American Society for Metals, Metals Park, OH, Vol. III, 1970, pp. 1031.

48. Kiyoshi Kusabiraki, Xiao-min Zhang and Takayuki Ooka, ISIJ International, 1995, Vol. 35(9), 1115.

49. P.W. Voorhees and W.C. Johnson, Phys. Rev. Let., 1988, Vol. 61(19), 2225.

50. K. Tsumuraya and Y. Miyata, Acta Metall., 1983, Vol. 31(3), 437.

51. W.C. Johnson, P.W. Voorhees and D.E. Zupon, Metal. Trans. 1989, Vol. 20A, 1175.

52. H.A. Calderon, P.W. Voorhees, J.L. Murray and G. Kostorz, Acta Metall., 1994, Vol. 42(3), 991.

53. T.L. Wolfsdorf, W.H. Bender and P.W. Voorhees, Acta Metall., 1997, Vol. 45(6), 2279.

54. R.A. Ricks, A.J. Porter and R.C. Ecob, Acta Metall., 1983, Vol. 31, 43.

55. C.H. Su and P.W. Voorhees Acta Metall., 1996, Vol. 44(5), 1987.

56. W.C. Johnson and P.W. Voorhees, J. Appl. Phy. 1987, Vol. 61(4), 1610.

57. W.C. Johnson, T.A. Abinandanan and P.W. Voorhees, Acta Metall., 1990, Vol. 38(7), 1349.

58. T.A. Abinandanan and W.C. Johnson, Acta Metall., 1993, Vol. 41(1), 17.

59. T.A. Abinandanan and W.C. Johnson, Acta Metall., 1993, Vol. 41(1), 27.

60. W. Hort and W.C. Johnson, Metall. and Mater Trans., 1994, Vol. 25A, 2695.

61. Y. Wang and A.G. Khachaturyan, Acta Metall., 1995, Vol. 43(5), 1837.

62. J.Y. Huh and W.C. Johnson, Acta Metall., 1995, Vol. 43(4), 1631.

63. C.H. Su and P.W. Voorhees Acta Metall., 1996, Vol. 44(5), 2001.

64. D.Y. Li and L.Q. Chen, Acta Mater., 1997, Vol. 45(6), 2435.

65. Y. Mou and J.M. Howe, Acta Mater., 1997, Vol. 45(2), 823.

66. M.E. Gurtin and P.W. Voorhees, Acta Metall., 1996, Vol. 44(1), 235.

67. F.R.N. Nabarro, C.M. Cress and P. Kotschy, Acta Metall., 1996, Vol. 44(8), 3189.

68. J. Svoboda and P. Lukas, Acta Metall., 1996, Vol. 44(6), 2557.

69. G. Solorzano, J. de Physique IV, 1993, Vol. 3(C7), 2021.

70. M. Tanaka, J. Mater. Sci., 1994, Vol. 29, 4093.

71. B. Radhakrishnan and R.G. Thompson, Metall Trans., 1993, Vol. 24A, 2773.

72. J. Friedel, Dislocations, (Pergmon Press New York, 1964), pp. 211.

73. J.C. Ion, K.E. Easterling and M.F. Ashby, Acta Metall., 1984, Vol. 32, 1949.

74. H.B. Aaron and G.R. Kotler, Metall. Trans., 1971, Vol. 2, 393.

75. Ercan Balikci, A. Raman, R. Mirshams, Z. Metallkunde, 1999, Vol. 90(2), 132.

76. D.A. Porter and K.E. Easterling, “Phase Transformations in Metals and Alloys”, 2nd ed., Chapman & Hall, New York, 1993, pp. 44-47, pp. 116, pp. 314.

77. Ercan Balikci, PhD Dissertation, pp. 51, LSU, Baton Rouge, LA , May 1998.

78. W. Ostwald, Analytische Chemie, 3rd edn., pp. 23., Engelmann, Leipzig, 1901.

79. R.E. Reed – Hill and R. Abbaschian, “ Physical Metallurgy Principles”, 3rd ed., Kent Publishing Co., Boston, 1992, pp. 256.

80. T. Miyazaki, H. Imamura and T. Kozaki, Mater. Sci. Engg., 1982, Vol. 54, 9.

81. R.A. MacKay and L.J. Ebert, Met. Trans., 1985, Vol. 16A, 1969.

82. A.G. Khachaturyan, S.V. Semenovskaya and J. W. Morris Jr., Acta Metall., 1986, Vol. 36, 1563

83. A.J. Ardell, R.B. Nicholson and J.D. Eshelby, Acta Metall., 1966, Vol. 14, 1295.

84. A.J. Ardell, Met. Trans., 1970, Vol. 1, 525.

Vita

Indranil Roy was born on August 17, 1972, in Asansol, West Bengal, India. After completing his Bachelor of Engineering in Mechanical Engineering in 1996, from Bengal Engineering College, India, he joined Group II, Heat Transfer Equipment Division of Larsen and Toubro Ltd., Mumbai, India. After working in Larsen and Toubro for almost 5 years, he came to the United States to pursue graduate studies in Spring 2001. He is pursuing his graduate education in the Department of Mechanical Engineering, Louisiana State University, Baton Rouge, Louisiana. He is currently a candidate for the degree of Master of Science in Mechanical Engineering to be awarded during the commencement of December 2003. After completing his master's degree he would be pursuing his doctoral program.